AD 741231

ARPA Order No. 1579 Amend. No. 2 Contract No. H0210008
Program Code No. 1F10
Contractor - Illinois Institute of Technology

Final Report

# Dynamic Photoelastic Analysis of Stress Wave Propagation due to a Distributed Line Charge

## Part I Full Plane

## Part II Quarter Plane

Details of illustrations in this document may be better studied on microfiche

Effective Date of Contract: Dec. 28, 1970
Contract Expiration Date: Dec. 28, 1971
Amount of Contract: $25,900
Principal Investigator: J. W. Dally
(301-454-2410)
Project Scientist: R. Prabhakaran
(301-454-2410)

Prepared for

U. S. Department of the Interior

Bureau of Mines

Twin Cities

Minnesota

Reproduced by
NATIONAL TECHNICAL
INFORMATION SERVICE
Springfield, Va. 22151

D D C
RECEIVED
5 MAY 1972
D

September 16, 1971

# DISCLAIMER NOTICE

THIS DOCUMENT IS THE BEST QUALITY AVAILABLE.

COPY FURNISHED CONTAINED A SIGNIFICANT NUMBER OF PAGES WHICH DO NOT REPRODUCE LEGIBLY.

Unclassified

3900.6 (Att 1 to Incl 1)
Nov 7, 66

DOCUMENT CONTROL DATA - R & D

Illinois Institute of Technology
3300 South Federal Street
Chicago, Illinois 60616

Unclassified

Dynamic Photoelastic Analysis of Stress Wave Propagation due to a Distributed Line Charge

Final Technical Report

James W. Dally, R. Prabhakaran

| | |
|---|---|
| 6. REPORT DATE: September 16, 1971 | 7a. TOTAL NO. OF PAGES: 66 / 7b. NO. OF REFS: 4 |
| 8a. CONTRACT OR GRANT NO.: H0210008 | 9a. ORIGINATOR'S REPORT NUMBER(S): H0210008 - 2 |
| b. PROJECT NO: 1579 | |
| c. Program Code 1F10 | 9b. OTHER REPORT NO(S) (Any other numbers that may be assigned this report): |
| d. Work Unit No. F53118 | |

10. DISTRIBUTION STATEMENT

Distribution of this document is unlimited.

| | |
|---|---|
| 11. SUPPLEMENTARY NOTES | 12. SPONSORING MILITARY ACTIVITY: Advanced Research Projects Agency, 1400 Wilson Boulevard, Arlington, Virginia 22209 |

13. ABSTRACT


Two series of dynamic photoelastic experiments utilizing line charges of lead azide are described. In the first series of tests, the stress waves generated in a full-plane model by three different ignition methods are investigated. Igniting the line charge at one end and igniting simultaneously at both ends result in comparable magnitudes of shear stresses and highly stressed regions. Center ignition of the line charge is the least effective method.

The second series of experiments is performed on photoelastic models of a quarter-plane where the distance between the line charge and the parallel free surface is varied for these tests, double-end ignition is employed. The reinforcement of the incident shear wave by reflected stress waves is studied and the effects of varying the spacing between the line charge and the free boundary are indicated.


DD FORM 1473

Unclassified

| KEY WORDS | LINK A ROLE | LINK A WT | LINK B ROLE | LINK B WT | LINK C ROLE | LINK C WT |
|---|---|---|---|---|---|---|
| Photoelasticity | | | | | | |
| Multiple dilatational sources | | | | | | |
| Stress waves | | | | | | |
| Multiple spark gap camera | | | | | | |
| Fringe patterns | | | | | | |
| Modeling | | | | | | |
| Explosives | | | | | | |

APRA Order No. 1579 Amend. No. 2 Contract No. H0210008

Program Code No. 1F10

Contractor - Illinois Institute of Technology

Final Report

# Dynamic Photoelastic Analysis of Stress Wave Propagation due to a Distributed Line Charge

## Part I Full Plane

## Part II Quarter Plane

by J. W. Dally and R. Prabhakaran

Prepared for

U. S. Department of the Interior

Bureau of Mines

Twin Cities

Minnesota

DDC

5 MAY 1972

DISTRIBUTION STATEMENT A

Approved for public release;

Distribution Unlimited

September 16, 1971

Sponsored by

Advanced Research Projects Agency

ARPA Order No. 1579, Amendment No. 2

Program Code No. 1F10

This research was supported by the
Advanced Research Projects Agency
of the Department of Defense and
was monitored by Bureau of Mines
under Contract No. H0210008

The views and conclusions contained in this document are those of the authors and should not be interpreted as necessarily representing the official policies, either expressed or implied, of the Advanced Research Projects Agency or the U.S. Government.

## TABLE OF CONTENTS


| | Page |
|---|---|
| ABSTRACT | iv |
| LIST OF TABLES | v |
| LIST OF ILLUSTRATIONS | vi |
| SECTION | |
| I. INTRODUCTION | 1 |
| II. EXPERIMENTAL PROCEDURE | 3 |
| III. FULL-PLANE EXPERIMENTS | 6 |
| IV. QUARTER-PLANE EXPERIMENTS | 32 |
| V. CONCLUSIONS | 56 |
| APPENDIX | |
| A. FRINGE PATTERNS | 59 |
| BIBLIOGRAPHY | 66 |

## ABSTRACT

Two series of dynamic photoelastic experiments utilizing line charges of lead azide are described. In the first series of tests, the stress waves generated in a full-plane model by three different ignition methods are investigated. Igniting the line charge at one end and igniting simultaneously at both ends result in comparable magnitudes of shear stresses and highly stressed regions. Center ignition of the line charge is the least effective method.

The second series of experiments is performed on photoelastic models of a quarter-plane where the distance between the line charge and the parallel free surface is varied for these tests, double-end ignition is employed. The reinforcement of the incident shear wave by reflected stress waves is studied and the effects of varying the spacing between the line charge and the free boundary are indicated.

## LIST OF TABLES

Page

TABLE

I. Comparison of the Shear Stress Regions sue to Different Ignition Procedures . . . 30

## LIST OF ILLUSTRATIONS


| Figure | | Page |
|---|---|---|
| 1. | Model Dimensions, in inches, for (a) Full-Plane and (b) Quarter-Plane Tests. | 4 |
| 2. | Typical Isochromatic Fringe Patterns for the Full-Plane Experiments. | 7 |
| 3. | Fringe Order as a Function of Position Along the Shear Normal for Single End Ignition of the Line Charge. | 11 |
| 4. | Fringe Order as a Function of Position Along the Normal to the P-wave for Single End Ignition of the Line Charge. | 12 |
| 5. | Development of Fringes in the Full-Plane with Single End Ignition. | 14 |
| 6. | Fringe Order as a Function of Position Along the Shear Normal for Center Ignition of the Line Charge. | 16 |
| 7. | Fringe Order as a Function of Position Along the Normal to the P-wave for Center Ignition of the Line Charge. | 17 |
| 8. | Fringe Order as a Function of Position Along the Normal to the Line Charge for Double End Ignition. | 19 |
| 9. | Interaction of Dilatational Waves due to Two Point Sources. | 20 |
| 10. | Early Development of Fringe Patterns in a Full-Plane for Double End Ignition. | 22 |
| 11. | Later Development of Fringe Patterns in a Full-Plane for Double End Ignition. | 23 |
| 12. | Variation of Fringe Order Along a Line 3 in. Distant From the Line Charge. | 26 |
| 13. | Comparison of the Shear Wave Intensities for the Three Ignition Procedures. | 28 |
| 14. | Regions Where the Fringe Order Due to the Shear Wave is Equal to or Greater Than 3.5. | 29 |
| 15. | Representative Fringe Patterns for the Quarter-Plane Test with $s = 6$ in. | 34 |
| 16. | Representative Fringe Patterns for the Quarter-Plane Tests with $s = 4.5$ in. | 35 |

17. Representative Fringe Patterns for the Quarter-Plane Test with s = 3 in. 36

18. Fringe Order on the Front Face as a Function of Position and Time (s = 6 in.). 39

19. Fringe Order on the Front Face as a Function of Position and Time ( s = 4.5 in.) 40

20. Fringe Order on the Front Face as a Function of Position and Time ( s = 3 in.) 41

21. Fringe Order Along the Normal to the Front Face for Selected Times ( s = 4.5 in.) 43

22. Selected Fringe Patterns Showing the Reflection Processes ( s = 4.5 in.) 44

23. Reinforcement of the Incident Shear (S) Wave by the Reflected Dilatational (PP) Wave. 46

24. Reinforcement of the Incident Shear (S) Wave by the Reflected Shear Waves (PS and SS), (s = 3 in.) 48

25. Fringe Order Along a Line 0.3 in. Below The Front Face as a Function of Position and Time ( s = 3 in.). 50

26. Maximum Fringe Order at the Front Face as a Function of the Distance Between the Front Face and the Line Charge (s). 52

27. Fringe Patterns Illustrating the Gradual Attenuation of Shear Wave for Double End Ignition. 53

28. Fringe Patterns Illustrating the Spatial Distribution of Shear Stress Maxima for Different Values of s. 55

A-1. Isochromatic Fringe Patterns for Single End Ignition of a Line Charge in a Full Plane. 60

A-2. Isochromatic Fringe Patterns for Center Ignition of a Line Charge in a Full Plane. 61

A-3. Isochromatic Fringe Patterns for Double End Ignition of a Line Charge in a Full Plane. 62

A-4. Isochromatic Fringe Patterns for the Quarter Plane Experiment with s = [illegible] in. 63

A-5. Isochromatic Fringe Patterns for the Quarter Plane Experiment with $s = 4.5$ in. 64

A-6. Isochromatic Fringe Patterns for the Quarter Plane Experiment with $s = 3$ in. 65

# I INTRODUCTION

The application of dynamic photoelasticity to the study of rock blasting techniques offers an experimental method which can adequately treat the complex phenomena involved. However, the use of dynamic photoelastic methods in this important problem area is very limited. Tandanand and Hartman[1]* have used a multiple spark camera to study fracture in glass and plastic plates impacted by a chisel-shaped tool. In the semi-annual technical report[2] of this continuing investigation, stress waves generated by multiple dilatational sources in a half-plane were examined in considerable detail. In this final report, stress waves due to line sources are examined in detail.

The interaction of the stress waves from a line charge of explosive with a bench face has been studied by Reinhardt and Dally[3]. They compared four different methods of igniting the line charge and concluded that simultaneous ignition at both ends was the most effective method.

In the present investigation, the generation and attenuation of stress waves due to various ignition procedures were studied in detail. A comparison of the ignition methods was made based on free propagation of stress waves in a full-plane. Next, the reflection and reinforcement of stress waves

---

* Numbered references are listed in the Bibliography

generated by a line charge near a free boundary were studied.

This study covers the results from three half-plane tests and three quarter-plane tests. A brief description of the experimental procedure employed is given in Section II of this report. The analysis of the data is presented in two parts. The first part, dealing with the half-plane experiments, is treated in Section III. The second part, which is treated in Section IV, deals with the quarter plane experiments. Finally, in Section V, conclusions are drawn from the present investigation and suggestions for future work are made.

## II EXPERIMENTAL PROCEDURE

The photoelastic models for the full-plane and quarter-plane experiments were fabricated from sheets of Columbia Resin CR-39. Grids with cross lines on 1-in. centers were scribed on the models after routing the edges. The charge in a bore hole was simulated by packing lead azide in a groove 6 inches long, 1/16 in. wide and 0.080 in. deep. The groove was machined in all the models on one face of the sheet on a milling machine. The groove was filled with 60 mg. of lead azide to the inch and ignited with bridge wire detonators.

In the series of experiments on the full-plane, three different ignition procedures were compared. In the first test, the charge was ignited at one end. In the second, the ignition was initiated at the center of the line charge. And in the third experiment, the line charge was ignited simultaneously at both ends by means of two bridge wire detonators whose resistances were closely matched. The model dimensions and groove location are shown in Fig. 1.

For the tests with the quarter plane, one of the ends of the groove was positioned 3 in. from one of the boundaries, the top face. The distance between the groove and the parallel boundary or the front face, denoted by s in Fig. 1, was varied in the three tests. The values of s used were 3,4.5 and 6 in.

The dynamic polariscope used in recording the photoelastic fringe patterns has been described in sufficient

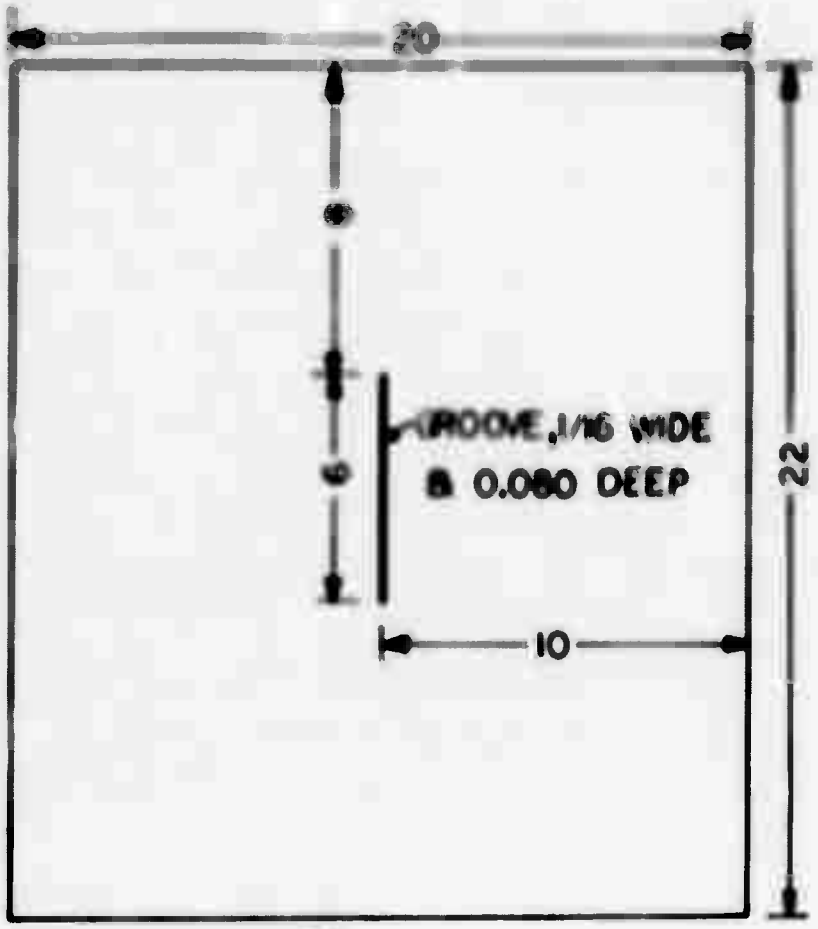


(A)

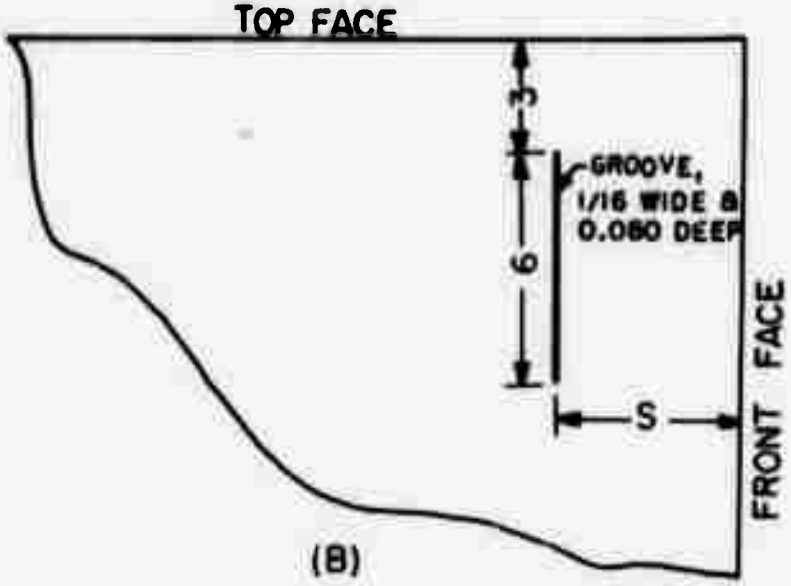


(B)

FIG. 1. MODEL DIMENSIONS, IN INCHES, FOR
(A) FULL PLANE & (B) QUARTER PLANE TESTS

detail in the previous report [2].

## III FULL-PLANE EXPERIMENTS

Three different methods of ignition of the line charge were compared by testing three photoelastic models. The models were large enough to avoid interaction with the boundaries. The line charges in these full-plane models were ignited at one end, at the center and at both ends, respectively. The resulting fringe patterns are shown in Figs. A-1, A-2 and A-3 in the appendix. Selected frames from the three tests are shown in Fig. 2. The frames have been selected so that the line charge was completely burnt and the fringe patterns were fully developed in each case.

The fringe pattern shown for single end ignition of the line charge corresponds to a time of 74 μsec. after the charge was ignited at the right end. Two distinct groups of fringes can be recognized, one due to the dilatational or P wave followed by the other due to the shear or S wave. The sets of fringes exhibit nearly plane fronts, whose inclinations to the line charge are donoted by angles $\alpha$ and $\beta$, for the P and the S waves, respectively. The wave speeds and the velocity of detonation of theline charge are related through these angles as

$$c_d = \frac{c_p}{\sin\alpha} = \frac{c_s}{\sin\beta} \qquad (1)$$

where $c_d$ is the velocity of detonation of the explosive

$c_p$ is the velocity of the P wave

and $c_s$ is the velocity of the shear wave.

The angles $\alpha$ and $\beta$ were measured as 38 and 20 degrees,

Reproduced from best available copy.

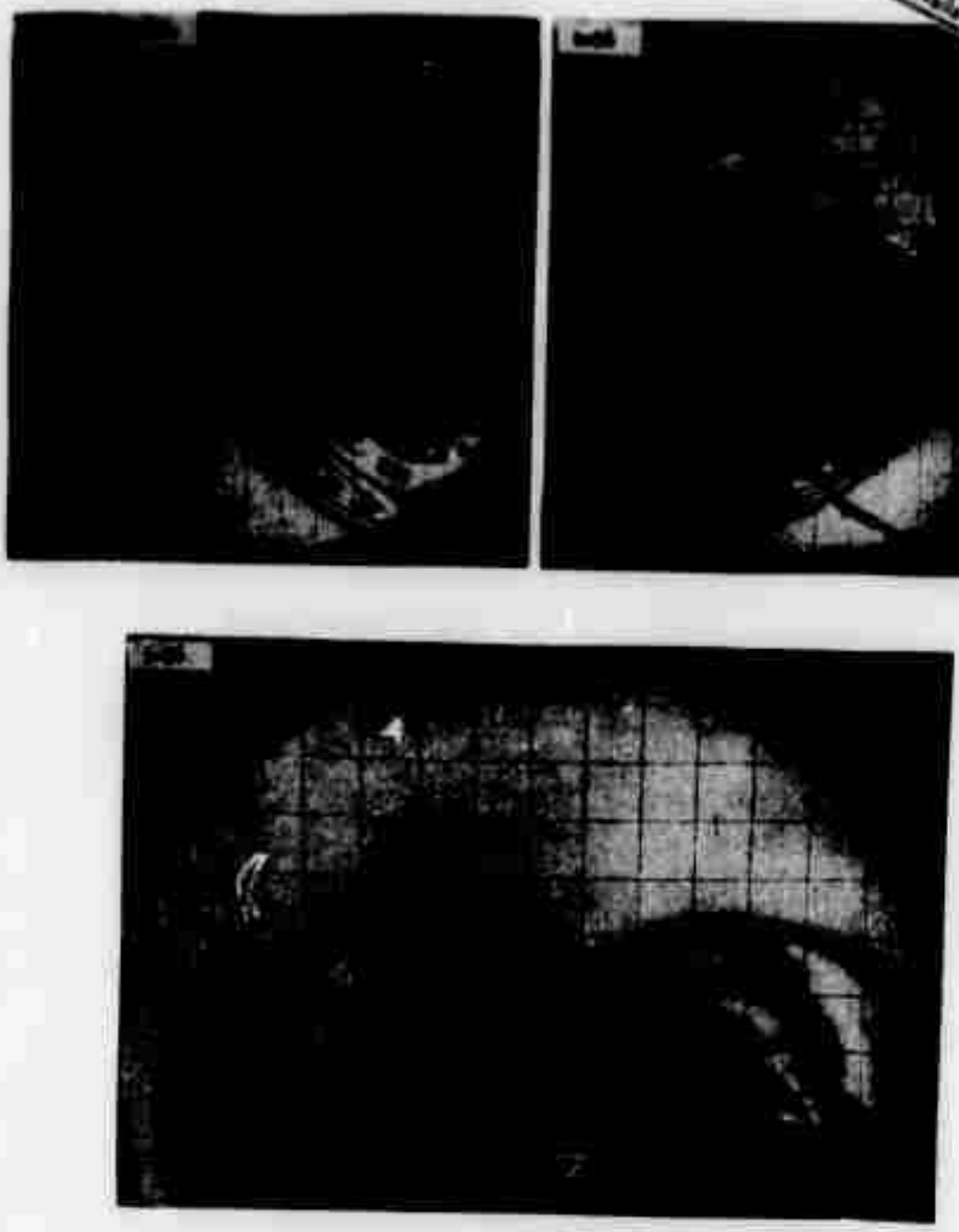

FIG.2 TYPICAL ISOCHROMATIC FRINGE PATTERNS FOR THE FULL-PLANE EXPERIMENTS

respectively, in the frame corresponding to 74 μsec. Taking values of 70,000 ips (in. per sec.) and 41,000 ips for the P and the S waves in CR-39, the velocity of detonation of the line charge in this experiment was 118,000 ips.

The fringe pattern for center ignition of the line charge, in Fig. 2, corresponds to a time of 56 μsec. after ignition. This fringe pattern is very similar to that due to single end ignition. In fact, center ignition of the 6 in. line charge can be considered equivalent to ignition at the common end of two 3 in. line charges placed end to end in a line. Again the P and the S waves can be observed with nearly plane fronts inclined at angles $\alpha$ and $\beta$ to the line charge, respectively. In this experiment, $\alpha$ was $40^{\circ}$ and $\beta$ was $22^{\circ}$, corresponding to a velocity of detonation of the line charge of 110,000 ips. This value is slightly less than the value measured for the case of end ignition, the difference in the velocities of detonation being due to the difference in the packing density of lead azide.

The isochromatic fringe pattern due to simultaneous ignition of the line charge at both the ends, shown in Fig. 2, corresponds to a time of 56 μsec. after ignition. This fringe pattern is different from the other two and can be visualized as the resultant of the interaction between two 3 in. line charges placed end to end and ignited at opposite ends simultaneously. The fringe pattern is symmetrical with respect to the perpendicular bisector of the line representing the explosive charge. The dilatational wave is followed by the shear wave as before. The two P waves due to the two 3 in.

line charges exhibit their individual characteristics on either side of the center line but have interacted near this line. The two S waves also have interacted with each other in the middle region but on either side they resemble the S wave due to single end ignition.

The fringe order, N, due to any of the stress waves is related to the difference in the principal stresses in the plane of the model by the stress optic law[4]

$$\sigma_1 - \sigma_2 = \frac{Nf_\sigma}{t} \qquad (2)$$

where $\sigma_1$ and $\sigma_2$ are the principal stresses

$f_\sigma$ is the material fringe value

and it is the model thickness.

In the fringe packet associated with the S (equivoluminal) wave, the first stress invariant must vanish. This requires that

$$\sigma_1 = -\sigma_2 = \frac{Nf_\sigma}{2t} \qquad (3)$$

so that the individual principal stresses can be found from the isochromatic fringe order, for the S wave.

(a) <u>Single end ignition</u>:

When the line charge is ignited at one end, the resulting P and S waves exhibit nearly plane fronts. The normals to these wave fronts are denoted by lines OA and O′B in Fig. 2 and are drawn perpendicular to the plane wave front through the point exhibiting the respective maximum fringe order. It is clear that each wave normal passes

through both the fringe packets but the maximum fringe order along any wave normal corresponds to the wave for which this line is the normal. For the frame in Fig. 2 shown for single end ignition, the maximum fringe order along the wave normal OA is 7 and the maximum fringe order along the wave normal O'B is also 7.

From the fringe patterns for single end ignition shown in Fig. A-1 in the appendix, the fringe orders along the two wave normals were measured as a function of position. The variation of the fringe order along the shear normal, OA, is shown in Fig. 3 for different times after the detonation of the explosive. It should be noted that the distances were measured along the wave normal starting from the point 'O' on the line charge. The position of point 'O' on the line charge thus shifted from frame to frame. The maximum fringe order, corresponding to the shear wave, drops from a value of 8.5 at a position 3 in. from the line charge (along the shear normal) to a value of 3 at a distance of 6.5 in.

The fringe orders corresponding to the dilatational wave are shown in Fig. 4 as a function of position along the wave normal O'B at different times. The maximum fringe order at a position 1.5 in. from the line charge (along the wave normal) is 8 and occurs at 65 μsec. The peak fringe order gradually decreases with increasing time and distance and drops to 3 at a distance of 9.5 in. at 152 μsec.

The burning of the line charge with one end ignited

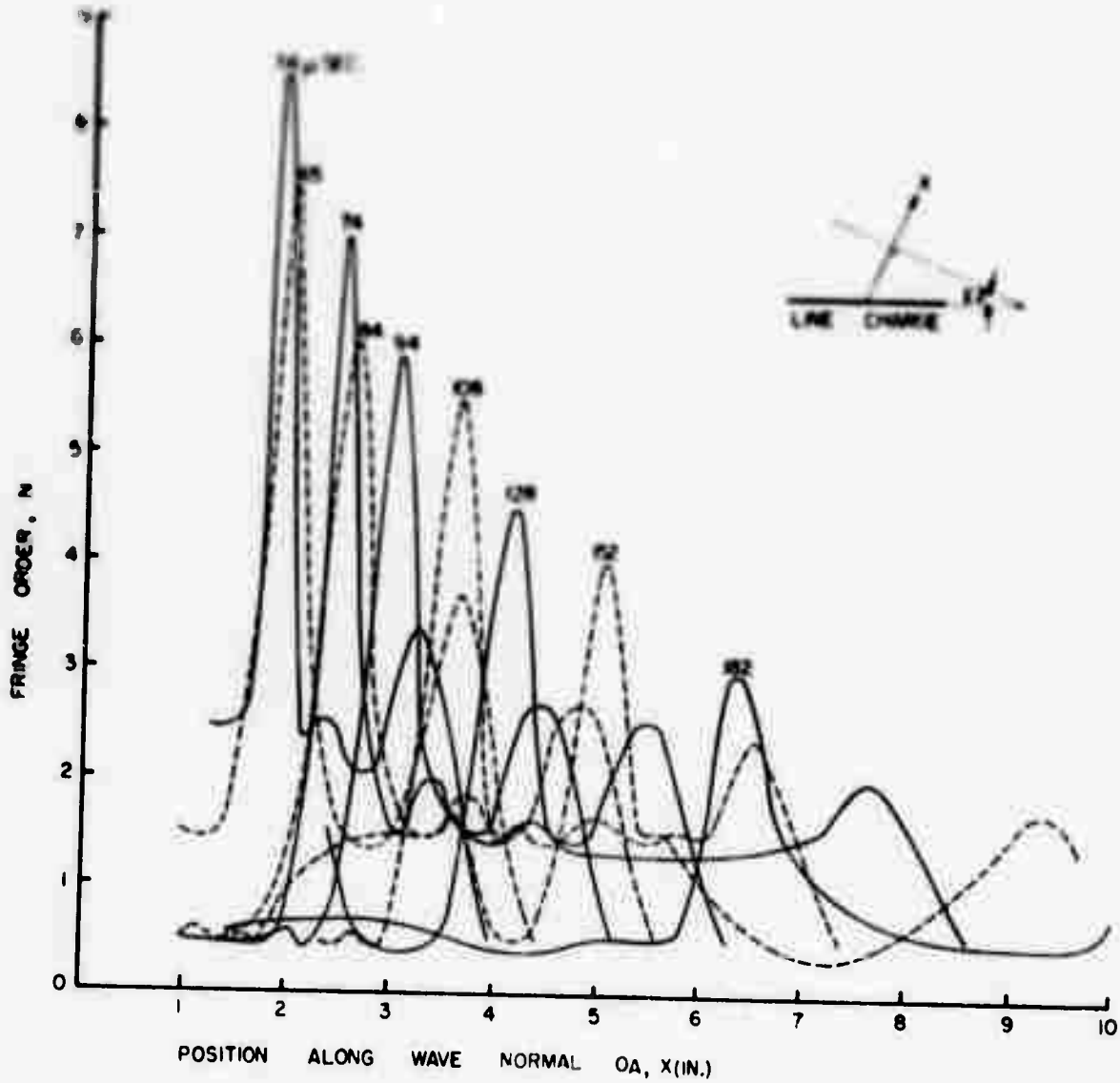


FIG. 3. FRINGE ORDER AS A FUNCTION OF POSITION ALONG SHEAR NORMAL FOR SINGLE END IGNITION OF THE LINE CHARGE

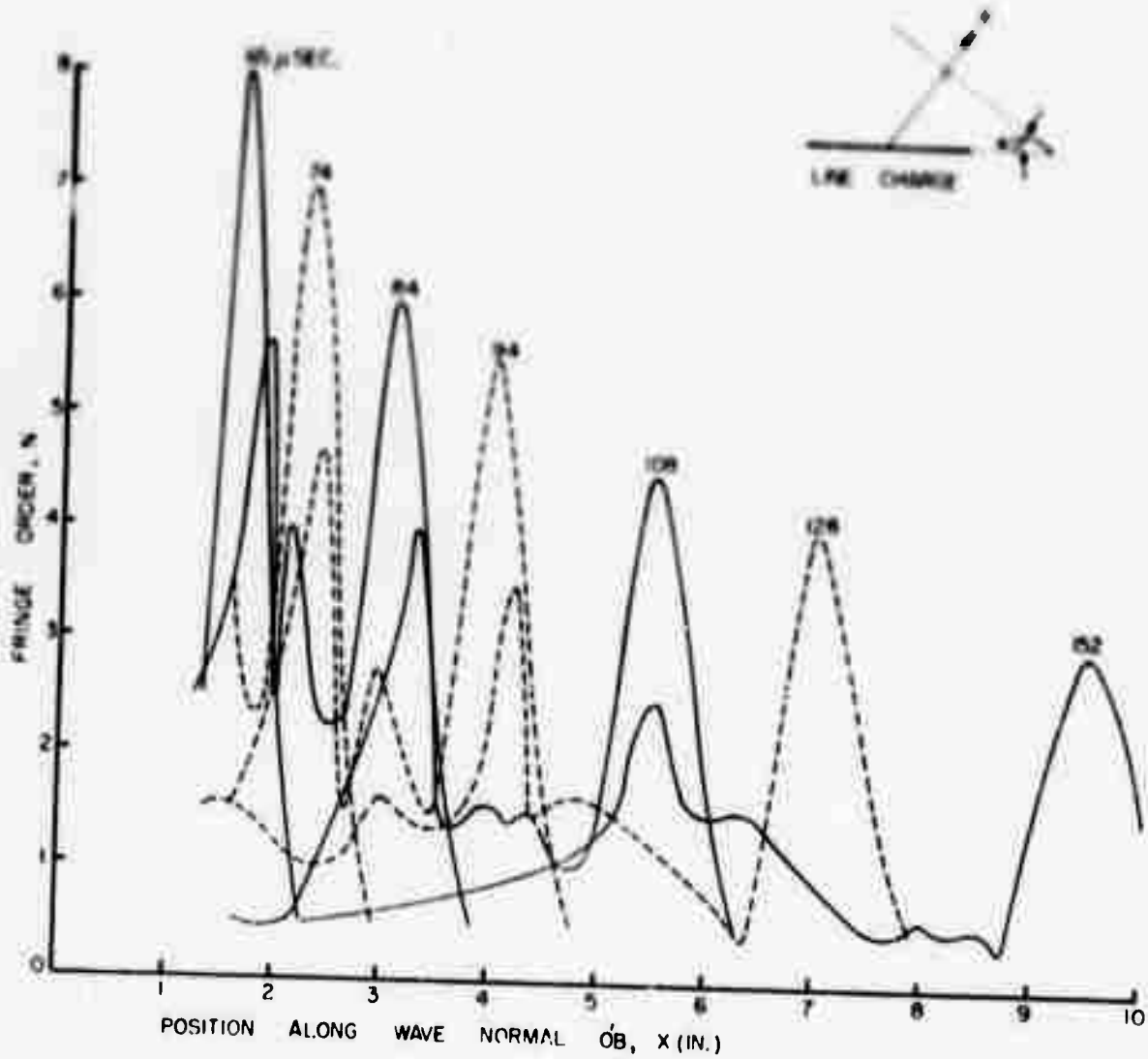


FIG. 4. FRINGE ORDER AS A FUNCTION OF POSITION ALONG THE NORMAL TO THE P-WAVE FOR SINGLE END IGNITION OF THE LINE CHARGE

can be considered to be equivalent to the ignition of a series of point sources in succession. Thus the stress waves due to each point source propagate and attenuate and are also reinforced by the stress waves generated by the successive point sources. The simultaneous attenuation and reinforcement makes it difficult to relate the time at which the peak intensity of the stress waves is reached to the burning time of the explosive. However, it is clear that for both the P and the S waves, the peak intensities should increase first and then decrease. This fact is illustrated in Fig. 5 where the development of the fringe patterns during the burning of the explosive is shown. The first two frames were taken at 38 and 46 μsec. and the explosive was only partially burnt. At 56 μsec. after ignition, the explosive was almost totally burnt, as shown by the third frame. The last frame corresponds to 65 μsec. when the fringe patterns were completely developed. For the P wave the maximum fringe order is 8 at 38 μsec., increases to 9 at 46 μsec. and 56 μsec. and then drops to 8 at 65 μsec. Of course, the maximum fringe order corresponding to the P wave could have been more than 9 at a time intermediate between 46 and 56 μsec. and peak may have been missed because no frames were recorded during this interval.

The peaks of the P wave and the S wave indicated in Figs. 3 and 4 show only the downward trend. The build-up of these fringe maxima is not shown because this build-up occurs in the early frames when the fringe gradients are very high for proper resolution and also the fringes are partially hidden by the smoke shield. However, it is to be expected that in

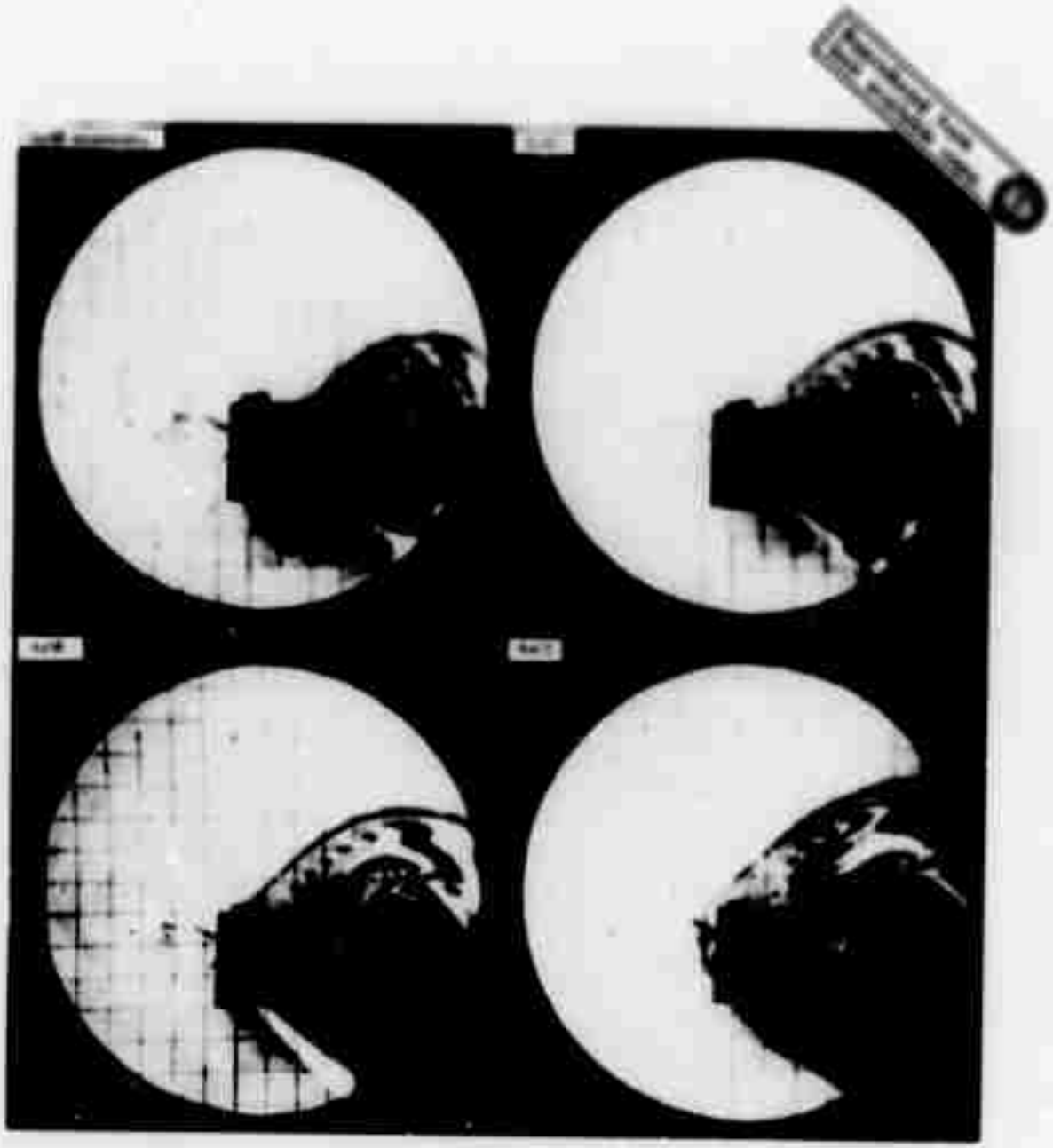

FIG.5 DEVELOPMENT OF FRINGES IN THE FULL-PLANE WITH SINGLE END IGNITION

the immediate vicinity of the explosive the stresses are very high and the material suffers damage. The magnitude of the stresses in regions away from the explosive are of more interest because extensive material damage is desired in mining applications. Therefore only the regions removed from the line charge need be considered in evaluating the effectiveness of the placement and ignition procedure for the line charge.

(b) Center ignition:

Due to the similarity between the fringe patterns resulting from single end ignition and center ignition, the comments made in connection with the wave normals in the previous section apply to the case of center ignition also. From the fringe patterns for center ignition shown in Fig. A-2 in the appendix, the variations of the fringe order along the two wave normals, shown in Figs. 6 and 7, were obtained.

The maximum fringe order due to the shear wave is 6.5 at a distance of 2 in. from the line charge (along the wave normal) and occurs at 56 usec. The dilitational wave exhibits a peak fringe order of 7 at a distance of 3.3 in. from the line charge corresponding to a time of 48 usec.

(c) Double end ignition:

When the line charge is ignited at both the ends simultaneously, the resulting fringe pattern is quite complex compared to the results due to the other two methods of ignition. The development of the fringe pattern from 22 usec. to 195 usec. is illustrated in Fig. A-3 in the appendix. As the fringe pattern is symmetrical about the line normal to

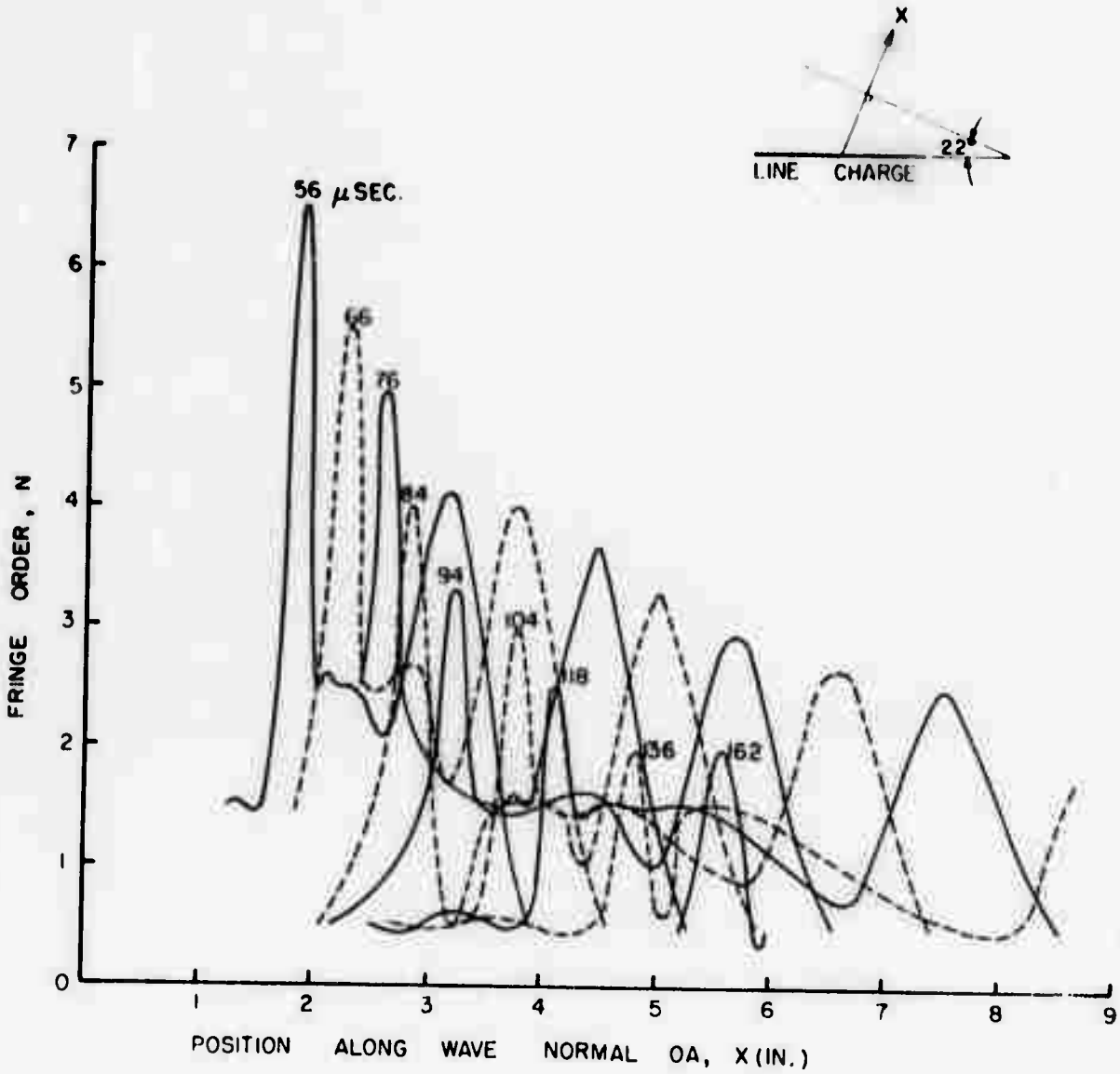


FIG. 6. FRINGE ORDER AS A FUNCTION OF POSITION ALONG THE SHEAR NORMAL FOR CENTER IGNITION OF THE LINE CHARGE

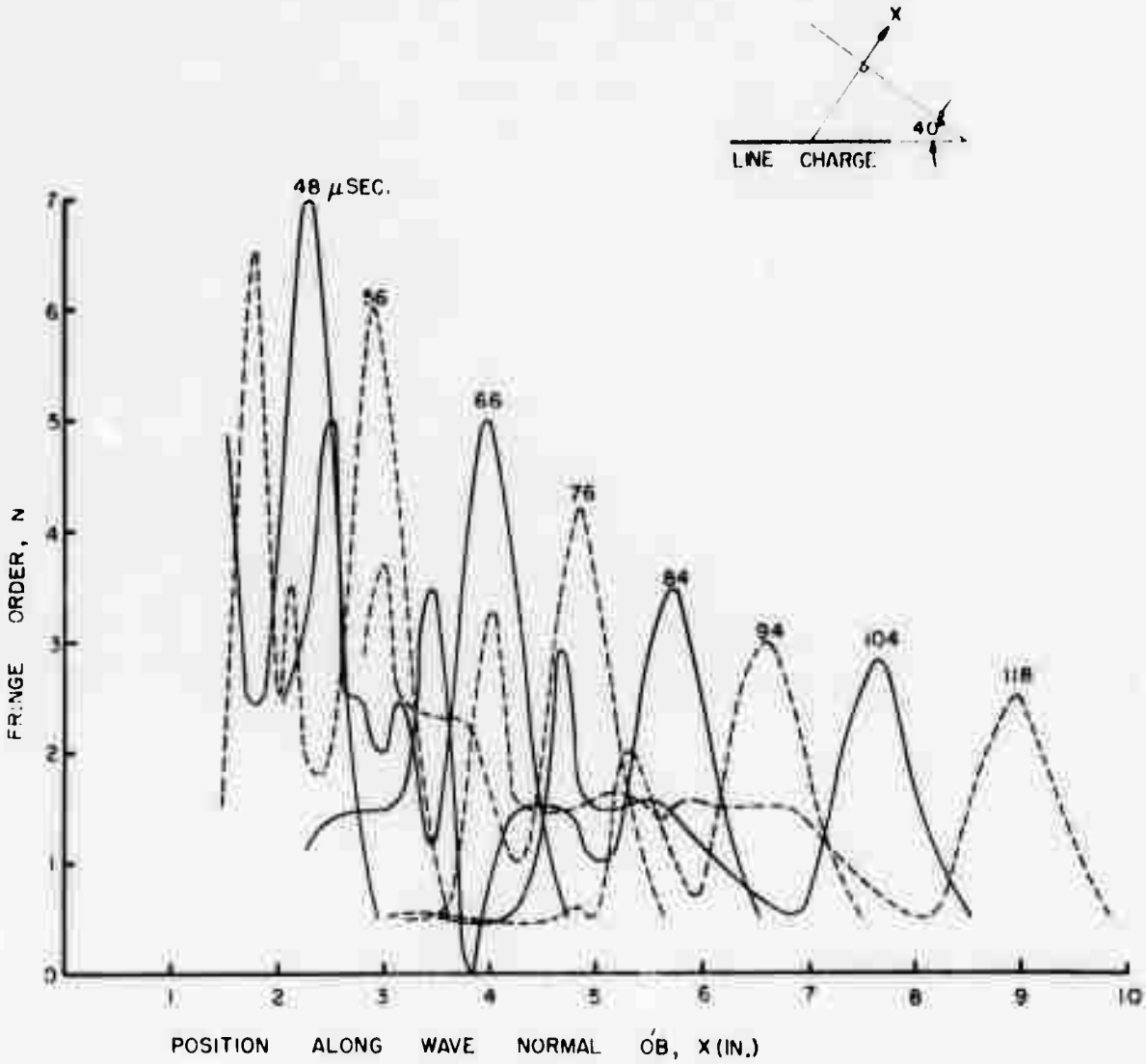


FIG. 7. FRINGE ORDER AS A FUNCTION OF POSITION ALONG THE NORMAL TO THE P-WAVE FOR CENTER IGNITION OF THE LINE CHARGE

the line charge at the middle, the fringe orders are shown as a function of position along the line of symmetry in Fig. 8. For clarity, the P wave fringe orders are shown below the position-axis.

The dilatational wave corresponds to a state of biaxial compression. As the isochromatic fringe order gives only the difference in the principal stresses, comparison of the P wave fringe orders does not give a comparison of the stress levels. This fact is illustrated in Fig. 9 where the P waves due to two point sources are shown reinforcing each other. The two wave normals are chosen, first, to be inclined at $45^{o}$ to the line of centers and therefore at right angles to each other. The state of stress on an element in the zone of reinforcement is shown in the figure. The subscripts for the stresses refer to the principal directions and the superscripts refer to the point source which is responsible for the stress component. It is clear that an isotropic state of stress is produced on the element resulting in zero isochromatic fringe order. The stress levels, however, are increased due to the reinforcement.

When the element under consideration is located on the line of centers, however, the difference in the principal stresses is doubled, resulting in a doubling of the isochromatic fringe order. The fringe order at any other point will be intermediate between these two extremes.

The interaction between the two P waves due to the two 3 in. halves of the line charge is more complex than the simple case of two point sources. However, the wave normal

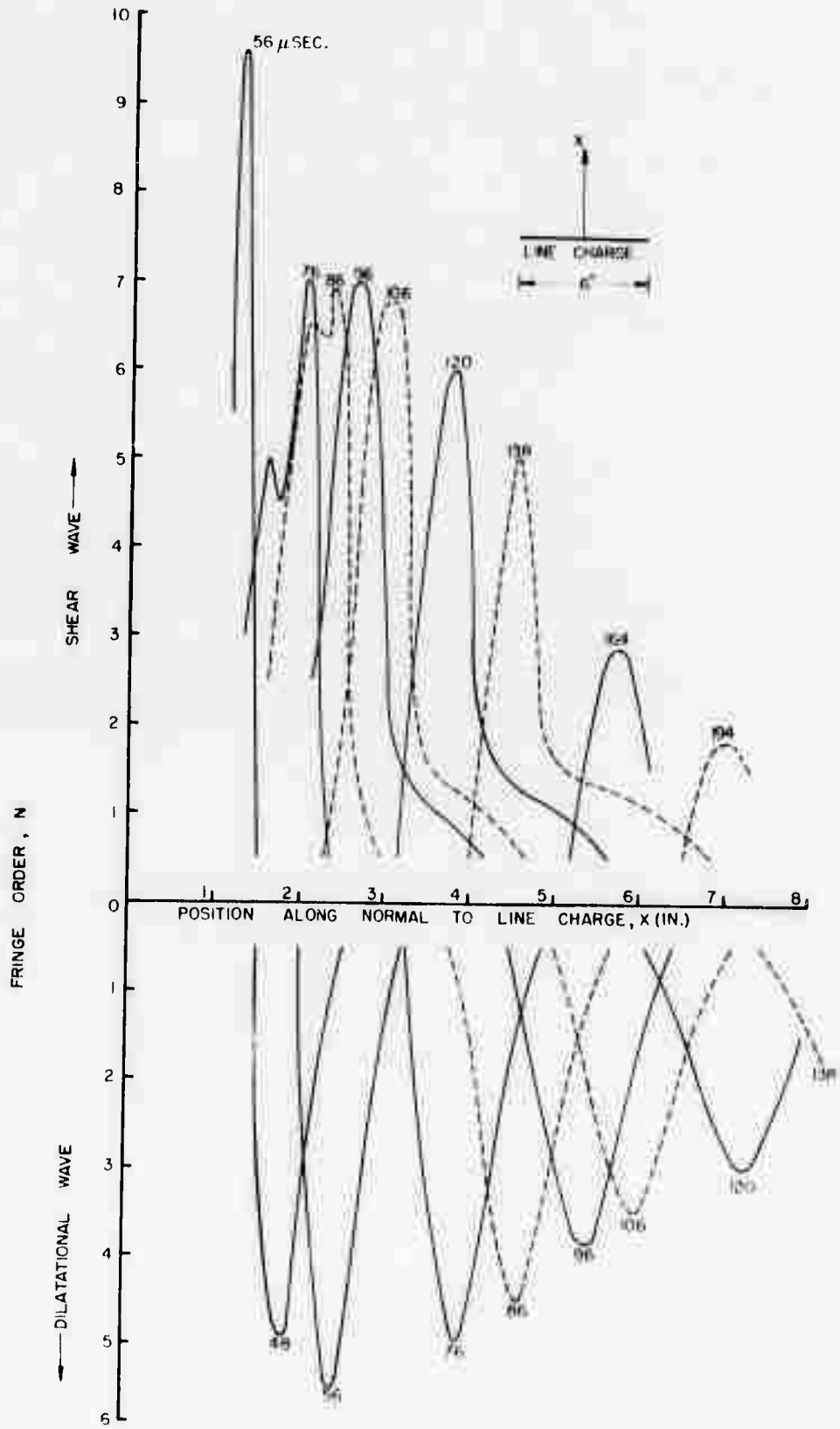


FIG. 8 FRINGE ORDER AS A FUNCTION OF POSITION ALONG THE NORMAL TO THE LINE CHARGE FOR DOUBLE END IGNITION

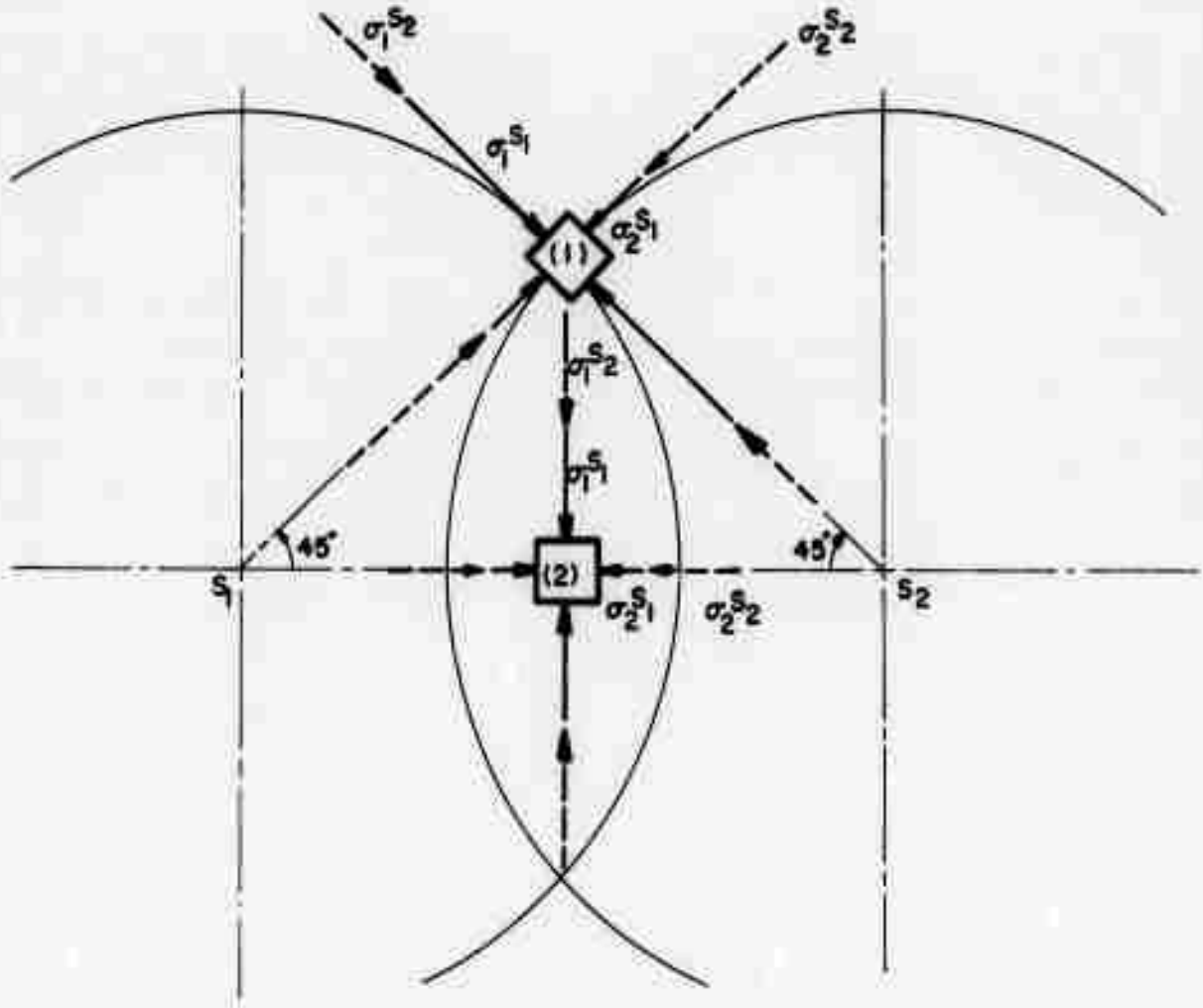


FOR ELEMENT (1), $N = 0$

FOR ELEMENT (2), $N = N^{S_1} + N^{S_2}$

FIG. 9. INTERACTION OF DILATATIONAL WAVES DUE TO TWO POINT SOURCES

for the P wave is inclined at about $40^{o}$ to the line charge and therefore conditions are closer to the case of the $45^{o}$ element described above. Thus there is a decrease in the isochromatic fringe order due to interaction although the individual principal stressss are raised in magnitude.

Selected frames showing the initial development of fringes are presented in Fig. 10. The first frame shows that at 25 μsec. the charge is not completely burnt. There are two unconnected sets of fringes, each due to single end ignition of a 3 in. line charge. The second frame at 34 μsec. shows that the burning is complete and the outer regions of the two sets of fringes have begun to interact. The inner regions of the two sets of fringes retain their characteristics of similarity to the single end ignition. The maximum fringe order, associated with the P wave, along the line of symmetry is only 4.5 whereas to either side of this line, P wave attains a maximum fringe order of 8. The frame at 40 μsec. shows that the P wave has attenuated considerably. The maximum fringe order on the line of symmetry is 4 and the maximum to either side of this line is 6.5. At 48 μsec., as shown in the last frame, the maximum P wave fringe order on the line of symmetry as well as to either side is close to 5. In the succeeding frames, shown in Fig. 11, the P wave exhibits its maximum fringe order over a region encompassing the line of symmetry and either side of this line.

The dilatational wave, producing a state of biaxial compression, is not effective in brea ing a brittle

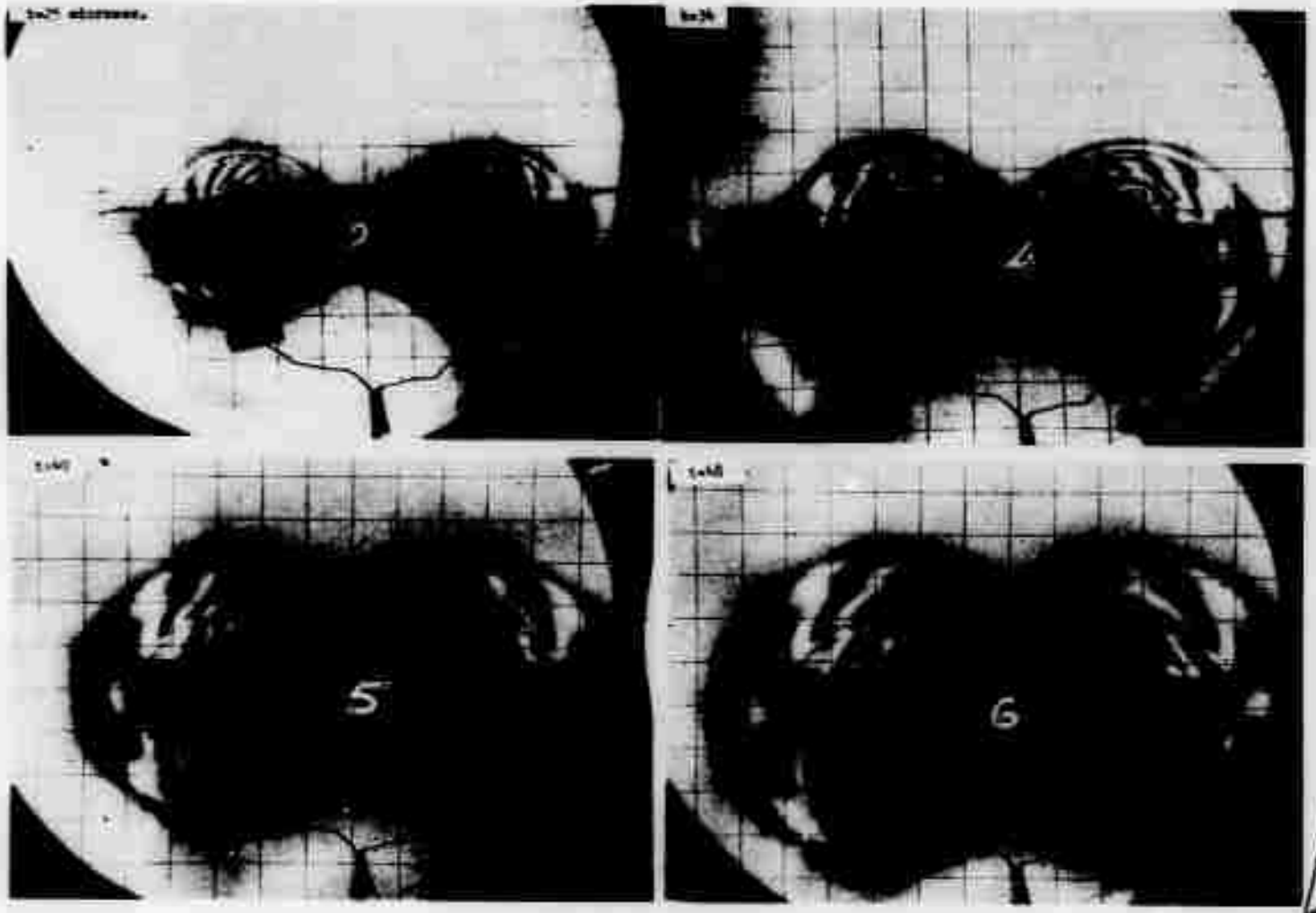


Reproduced from best available copy.

FIG.10 EARLY DEVELOPMENT OF FRINGE PATTERNS IN A FULL -PLANE FOR DOUBLE END IGNITION

FIG.11 LATER DEVELOPMENT OF FRINGE PATTERNS IN A FULL-PLANE FOR DOUBLE END IGNITION

material such as rock whose compressive strength is many times the tensile strength, except when the P wave is reflected from a free boundary and the compressive stresses are converted to tensile stresses. Therefore, the shear wave, which produces equal tension and compression, is more significant in the full-plane experiments. The variation of the fringe order associated with the shear wave along the axis of symmetry is shown in Fig. 8. The shear wave exhibits a maximum of 9.5 fringes at a distance of 1.3 in. from the line charge. This high fringe order is due to the reinforcement of the two S waves from the two halves of the line charge and is beneficial in rock breakage. The selected fringe patterns shown in Fig. 11 clearly illustrate the interaction between the two shear waves due to the two halves of the line charge. At 56 μsec., as illustrated by the first frame, the two shear waves have interacted in the middle (near the line of symmetry) but still exhibit their individual characteristics on either side. The maximum fringe order is 9.5, both at the middle as well as at either side of the center. In the frame corresponding to 76 μsec. the two individual incident shear waves are difficult to recognize as interaction is more extensive. The maximum fringe orders on the line of symmetry and on either side of it are the same and equal to 6.5. At 96 μsec. the maximum fringe order at center is 7 while on either side it is only 6. In succeeding frames, the shear wave peak occurs on the line of symmetry only, as clearly evident from the frame at 106 μsec.

The variation of fringe order along a line 3 in. distant from the line charge is shown in Fig. 12. The increase in fringe order between 48 μsec. and 66 μsec. is due to the incident P wave. As the P wave passes through the line under consideration, the fringe order drops from 66 μsec. to 86 μsec. Between 86 μsec. and 106 μsec. the fringe order increases rapidly due to the shear wave. Thereafter there is a steep decrease in the fringe order as the crests of the stress waves pass beyond the line.

The peaks at 66 μsec. occur at two points on the line parallel to the line charge and are due to the crest of the P wave. The maximum fringe order at 106 μsec. occurs over a localized region at the center and is due to the shear wave. These two curves illustrate the phenomenon already mentioned, namely that after the interaction of the stress waves from the two halves of the line charge is complete, the crest of the P wave is spread out whereas the crest of the shear wave is localized.

Comparison of the Three Methods of Ignition:

The objective of the full plane experiments was to study the interaction and reinforcing process when a line charge was ignited in the three different ways. The three ignition procedures can be compared on the basis of the maximum isochromatic fringe order corresponding to the shear wave and on the basis of the extensiveness of the high shear stress regions. The isochromatic fringe order corresponding to the dilatational wave are not meaningful for the comparison because these fringes are associated with a state of

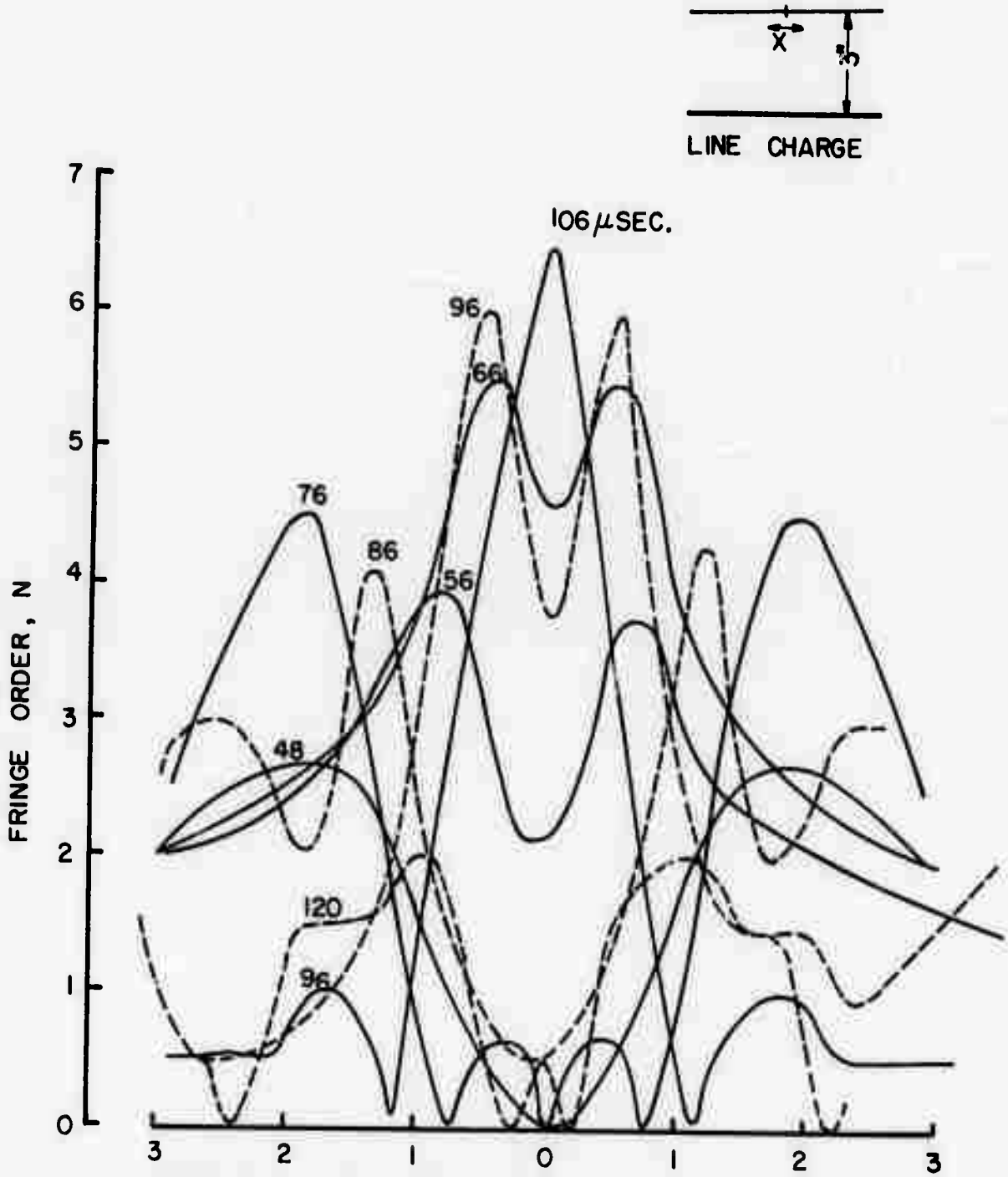


FIG. 12. VARIATION OF FRINGE ORDER ALONG A LINE 3" DISTANT FROM THE LINE CHARGE

biaxial compression which is not significant in producing damage in brittle materials.

The maximum values of the isochromatic fringe order corresponding to the shear wave are shown for the three methods of ignition in Fig. 13 as a function of the distance from the line charge. This figure is derived from Figs. 3, 6, and 8. It should be noted that in the case of single end ignition and center ignition the distances are measured along the shear wave normal. The fringe order peaks for the center ignition are well below the values for the other two ignition procedures. Between 2.5 in. and 5 in. double end ignition produces higher shear stresses than single end ignition but beyond 5 in. the reverse is true.

As mentioned before, in addition to the stress intensities, the extensiveness of the high stress regions are also important in comparing the various ignition procedures. The regions in which the fringe order due to the shear wave is equal to or greater than 3.5 for the three full-plane experiments are shown in Fig. 14. Only half of the regions are shown because of symmetry about the line charge. The areas were obtained by tracing the shape of the N = 3.5 fringe order at different times and enclosing the fringes in an envelope. The areas indicated are those beyond 1 in. from the line charge. The area for center ignition is 0.53 times that for single end ignition and for the double end ignition the area is 1.08 times the value for single end ignition. The areas corresponding to N = 2.5 and N = 4.5 were also determined and the results are summarized in Table I.

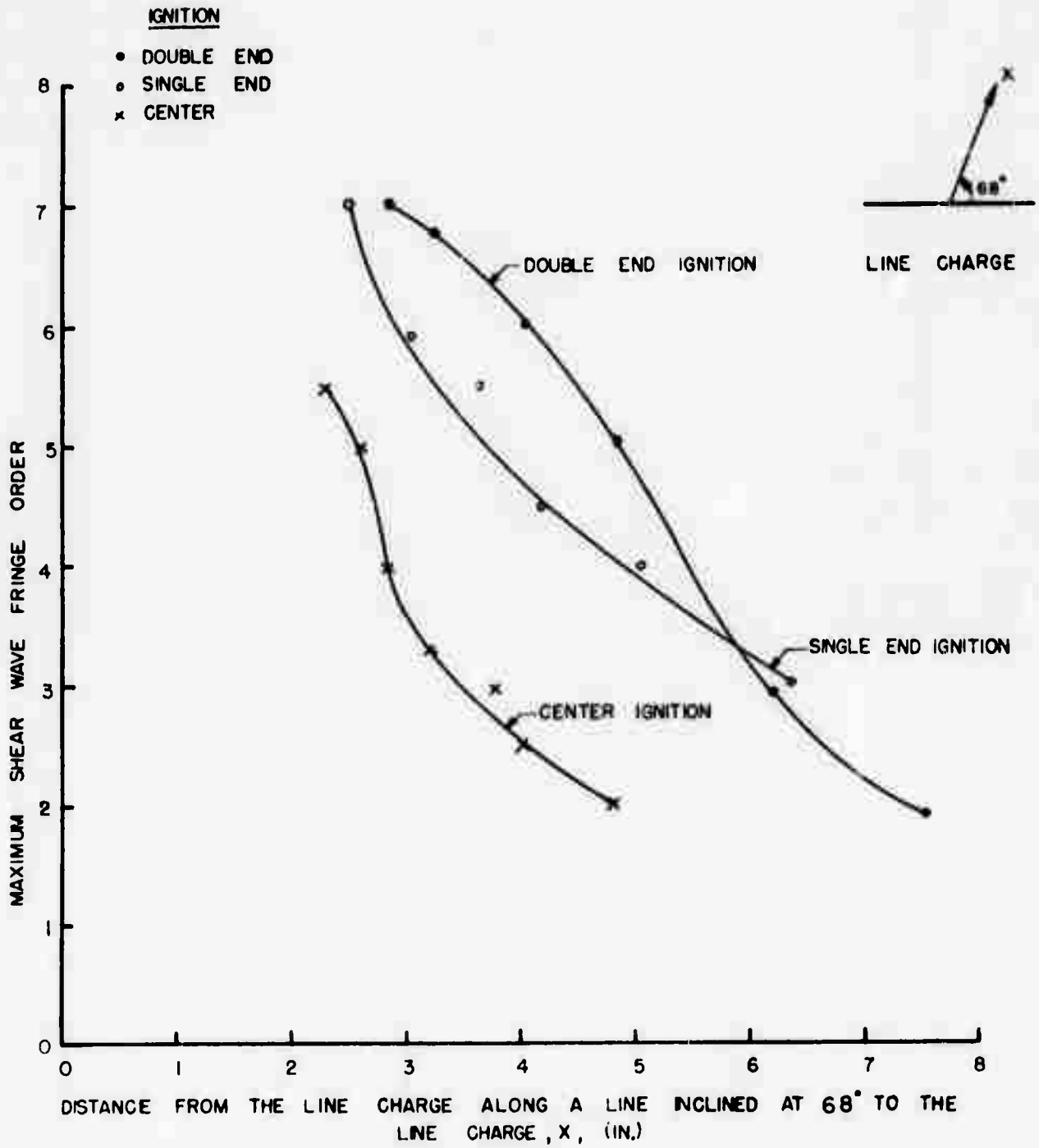


FIG. 13. COMPARISION OF THE SHEAR WAVE INTENSITIES FOR THE THREE IGNITION PROCEDURES

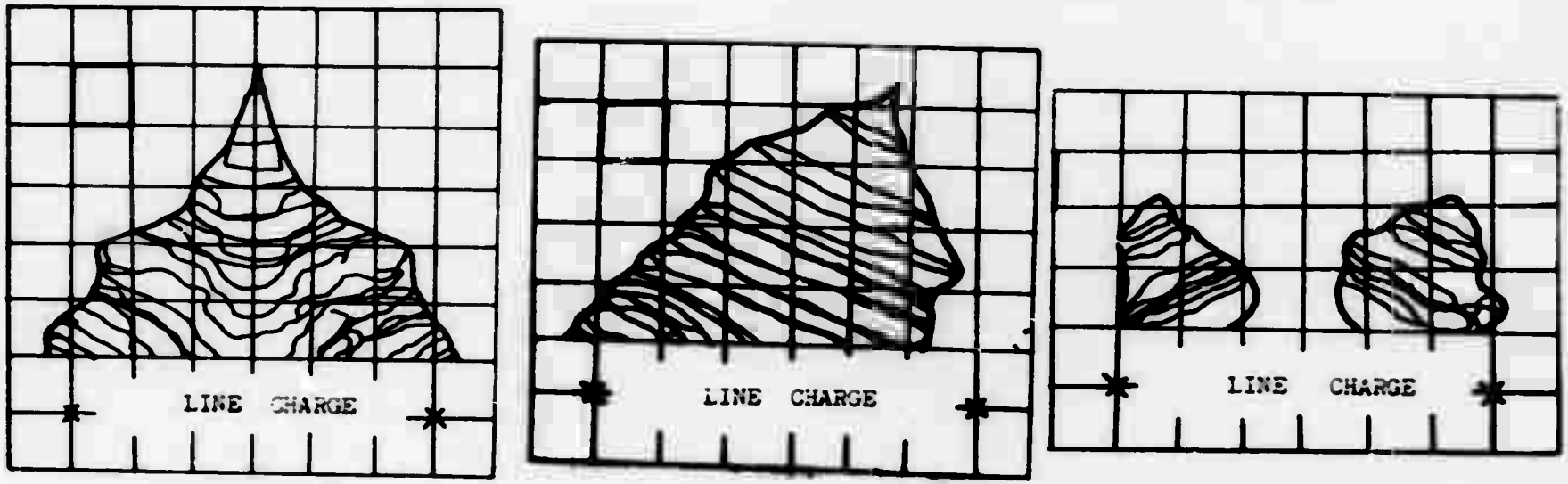


AREA=15.5 in.$^2$
DOUBLE END IGNITION

AREA=14.3 in.$^2$
SINGLE END IGNITION

AREA=7.6 in.$^2$
CENTER IGNITION

FIG.14 REGIONS WHERE THE FRINGE ORDER DUE TO THE SHEAR WAVE IS EQUAL TO OR GREATER THAN 3.5

Table I

Comparison of the Shear Stress Regions due to Different Ignition Procedures

| Fringe order N | $\frac{A_{de}}{A_{se}}$ | $\frac{A_c}{A_{se}}$ |
|---|---|---|
| 2.5 | 0.95 | 0.56 |
| 3.5 | 1.08 | 0.53 |
| 4.5 | 1 | -- |

de: double end ignition
se: single end ignition
c: center ignition

Single end ignition and double end ignition are almost equally effective in producing highly stressed regions and center ignition is only half as effective.

In summary, center ignition is the least effective ignition procedure. Single end ignition and double end ignition are comparable in their effectiveness both in terms of the magnitude of the shear stresses and in terms of the areas of high shear stress. The ignition procedures could not be compared on the basis of the dilatational wave because the isochromatic fringes give only the principal stress differences; besides, the biaxial compressive state of stress due to the dilatational wave is not significant in producing fracture in materials with low tensile strength.

In the next chapter, quarter-plane experiments are

described in which the double end ignition was employed. In these experiments, reflections from a boundary parallel to the line charge were studied. For this particular orientation, Reinhardt and Dally[3] have found that double end ignition produces higher tensile stresses at the boundary compared to single end ignition or center ignition. For other rientations of the free boundary, with respect to the line charge, single and double end ignition procedures will have to be compared to judge which is more effective.

# IV QUARTER-PLANE EXPERIMENTS

The results from the full-plane experiments have shown that, of the three ignition procedures studied, center ignition of the line charge is the least effective. Igniting at one end and at both ends produce comparable effects, both in terms of the shear stress magnitudes and the extensiveness of the high shear stress regions. Although the P wave was not considered a significant factor for comparison in the full-plane experiments, it assumes a prominent role when reflections from free boundaries are of interest, because of the reflected P (PP) and reflected shear (PS) waves. Reinhardt and Dally[3], in their dynamic photoelastic study of a bench face, compared different ignition procedures and concluded that simultaneous ignition at both ends was the most effective technique. In the quarter plane experiments described in this Chapter, where the line charge was parallel to one of the free boundaries, double end ignition was employed.

The photoelastic models employed in the series of experiments are schematically shown in Fig. 1. The two free boundaries of the quarter plane are labelled top face and front face. The line charge was positioned parallel to the front face with one end of the line charge 3 in. from the top face. The distance between the line charge and the front face, denoted by s in Fig. 1, was varied. Four photoelastic models were tested, with values of 6, 4.5, 3 and 1.5 in. for s. In the case of 1.5 in. spacing, the number of fringes

and the fringe gradients were so high that fringe resolution was not adequate. Hence only the results for the other three experiments are reported here.

A set of sixteen fringe patterns for each quarter plane experiment is given in the Appendix in Figs. A-4, A-5 and A-6. In each case, the photographic record was started just when the incident stress waves reached the boundary. The timing between the frames was adjusted to obtain photographs of the interaction process until the reflections were essentially complete. Selected fringe patterns from each of the three tests are shown in Figs. 15 and 16 and 17. The first frame, taken at 80 μ sec., shows the undistorted shape of the incident waves prior to interaction with the front face. At this time, the two groups of stress waves due to the two halves of the line charge have interacted with each other. Also, interaction with the top face has occurred. The next frame, at 122 μ sec. shows the result of the interaction of the incident P wave with the front face. The incident P wave has produced two waves upon reflection, the PP or reflected dilatational wave and the PS or reflected shear wave. In the second frame, the PP wave is reinforcing the incident shear or S wave at about 2 in. from the front face. The PS wave has travelled about 1 in. away from the boundary. In the third frame, corresponding to 130 μ sec., the PS wave is reinforcing the S wave at about 1.5 in. from the front face. In the final frame, at 171 μ sec., the PS wave and the S wave have crossed each other, the former travelling about midway to the line charge and the crest

FIG.15 REPRESENTATIVE FRINGE PATTERNS FOR THE QUARTER-PLANE TEST WITH s=6 in.

Reproduced from best available copy.

FIG.16 REPRESENTATIVE FRINGE PATTERNS FOR THE QUARTER-PLANE TEST WITH s=4.5 in.

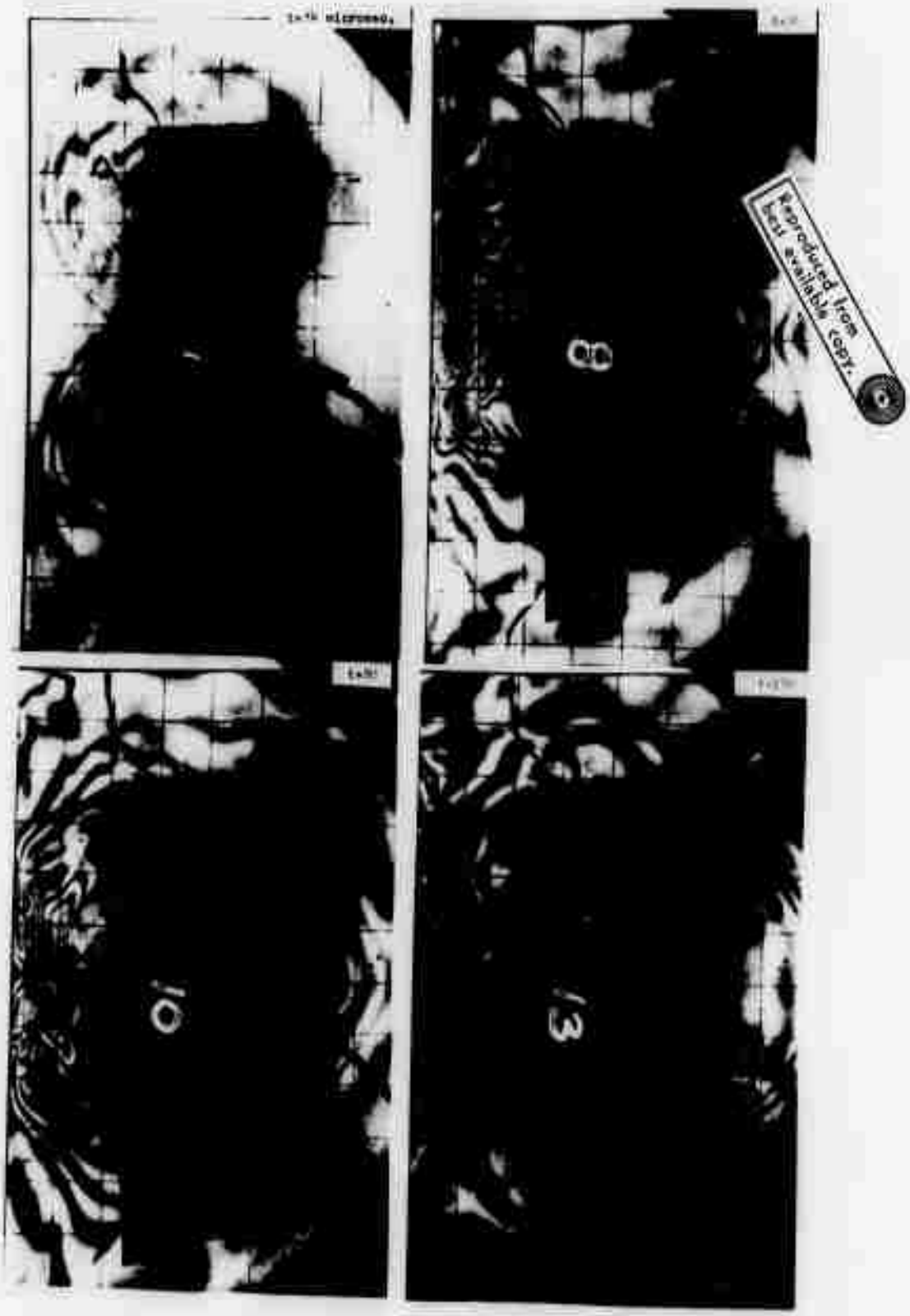


Reproduced from best available copy.

FIG.17 REPRESENTATIVE FRINGE PATTERNS FOR THE QUARTER-PLANE TEST WITH s=3 in.

of the latter reaching the front face.

The important features in the reflection of stress waves when s = 4.5 in. are illustrated in Fig. 16. The reflection process follows essentially the same pattern as that described for s = 6 in. except that now the corresponding events occur at shorter times and the amplitudes of the stress waves involved are higher. Both these differences are due to the shorter spacing between the line charge and the front face.

Selected frames from the test for s = 3 in. are presented in Fig. 17. The fringe patterns are more complex compared to the other two cases, because of the higher fringe orders and fringe gradients involved. In the first frame, taken at 34 μ sec., the incident stress waves are about to reach the front face. The second frame shows a complicated fringe pattern with many fringe order peaks and valleys. The P wave has produced the PP and the PS wave at this time. The PP wave has interacted with the incident shear wave, S, and the PS wave has travelled about 0.3 in. away from the boundary. At 80 μ sec., as shown in the third frame, the PS wave is reinforcing the S wave. In the final frame, corresponding to 100 μsec., the PS wave has travelled half way towards the line charge and the S wave is interacting with the front face. In the right half of the photograph the S wave exhibits a maximum fringe order of 8 whereas the maximum fringe order at the front face is 10. The increase of two fringe orders at the free boundary is due to the reinforcement of the S wave by the reflected shear wave, SS.

The fringe order along the front face for the three

quarter plane experiments is presented for different times in Figs. 18, 19 and 20. When the spacing between the line charge and the front face is 6 in., Fig. 18 shows that the fringe order at the point on the boundary directly in line with the center of the line charge is negative between 114 and 130 μsec., indicating a compressive state of stress in the tangential direction. At later times the stress at this point becomes increasingly tensile as shown by the curves for 140, 156, 162 and 171 μsec. The stress peaks move towards the center from both sides till a maximum fringe order of 4 is reached at 171 μsec. This maximum of 4 fringes is due to the reinforcement of S wave by the SS wave. The asymmetry in the fringe order-position curves is due to the difference in the amount and packing density of the explosive in the two halves of the line charge. From the first frame in Fig. 15, the fringe pattern before the stress waves have started interacting with the front face is asymmetrical and this asymmetry persists later. After the stress reaches the peak on the front face, the fringe order peaks start decreasing and moving to either side of the center.

The fringe order-position curves for 4.5 in. spacing are shown in Fig. 19. These variations exhibit the same characteristics as those for s = 6 in. The maximum fringe order at the center is now 8, attained at 132 μsec., and is again due to the reinforcement of the incident shear or S wave by the reflected shear or SS wave.

The variation of fringe order along the front face when s = 3 in. is shown in Fig. 20. The reinforcement of the

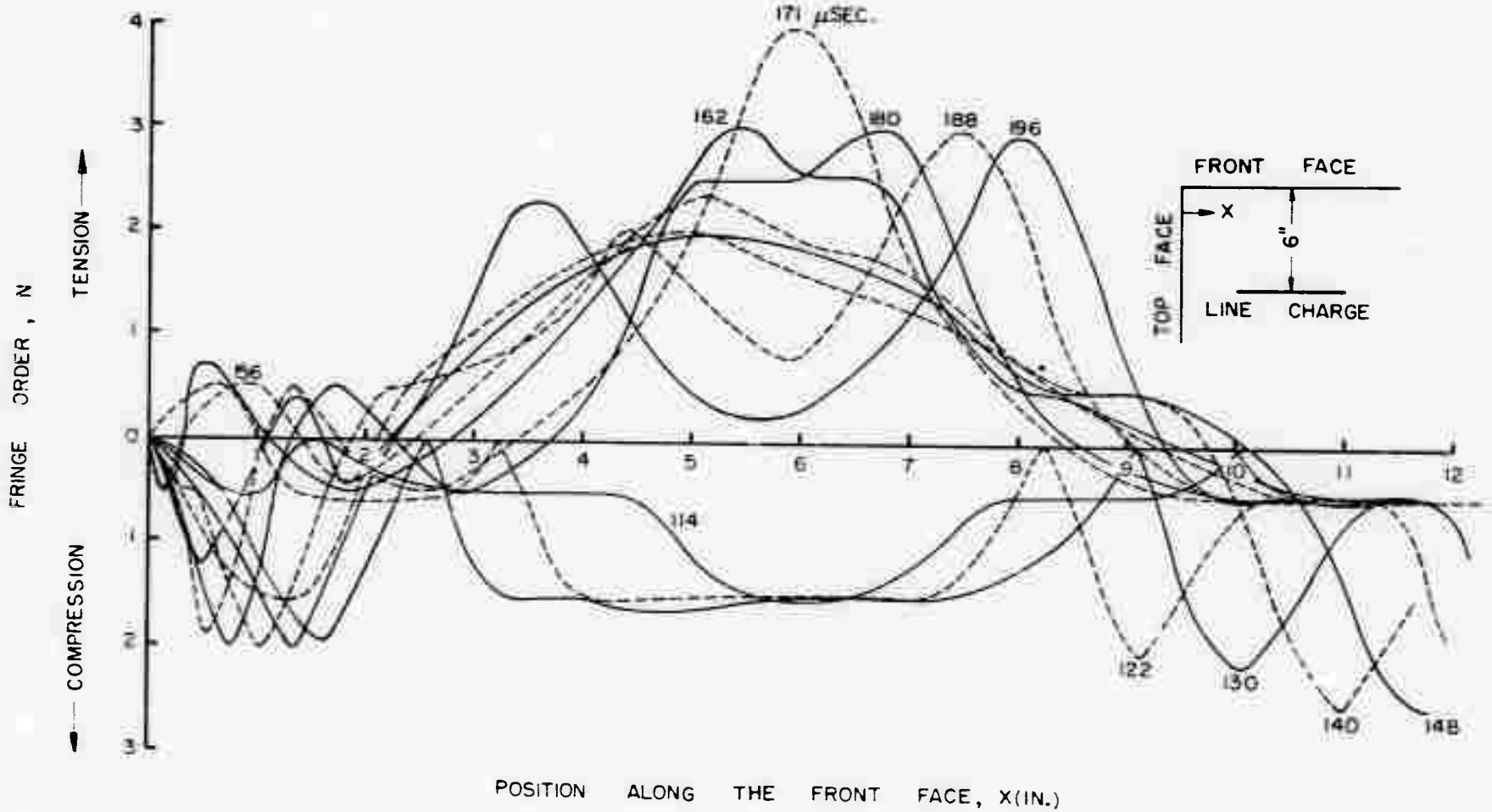


FIG. 18. FRINGE ORDER ALONG THE FRONT FACE AS A FUNCTION OF POSITION AND TIME (s = 6 IN.)

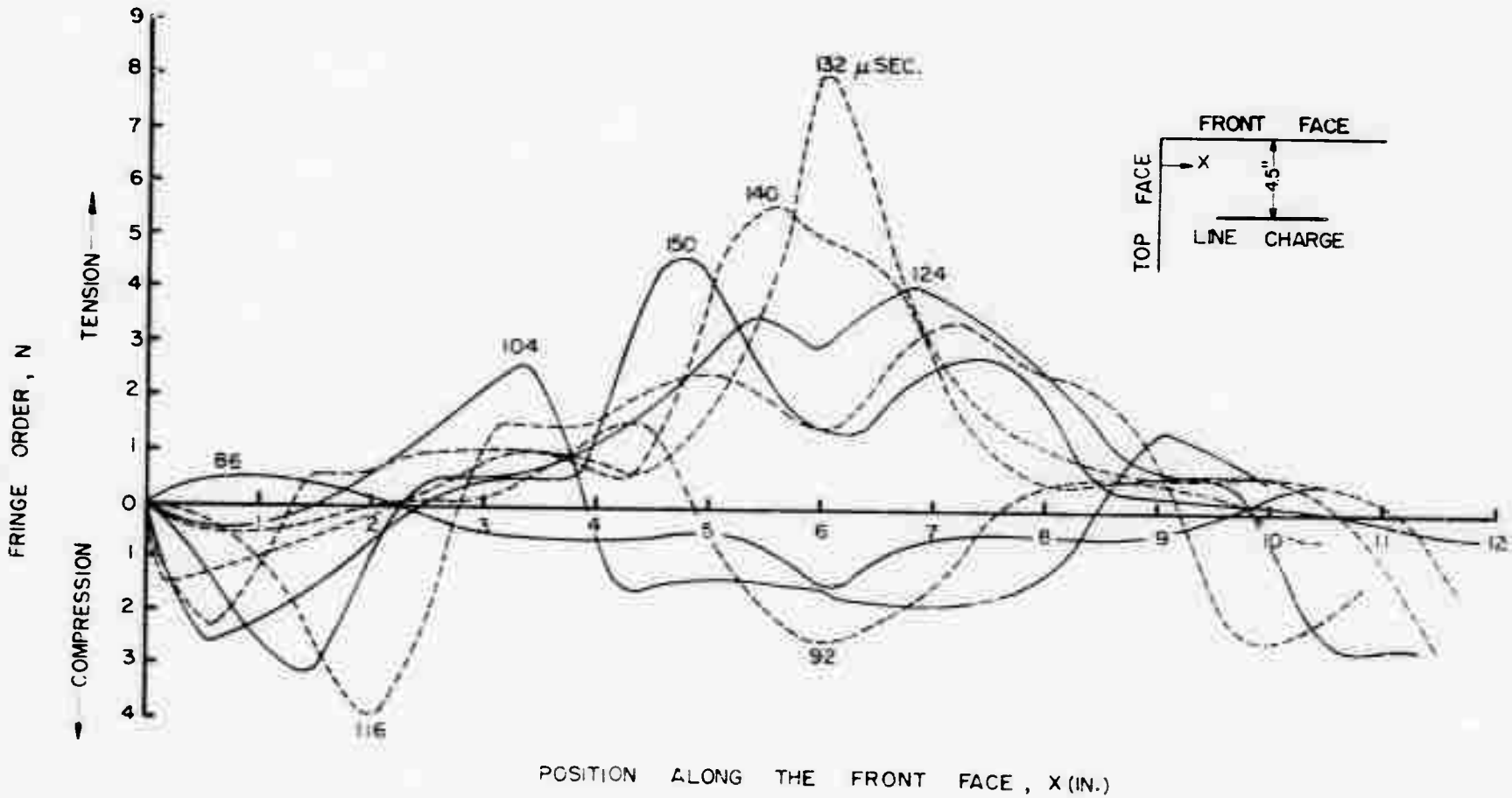


FIG. 19. FRINGE ORDER ALONG THE FRONT FACE AS A FUNCTION OF POSITION AND TIME (s = 4.5 IN.)

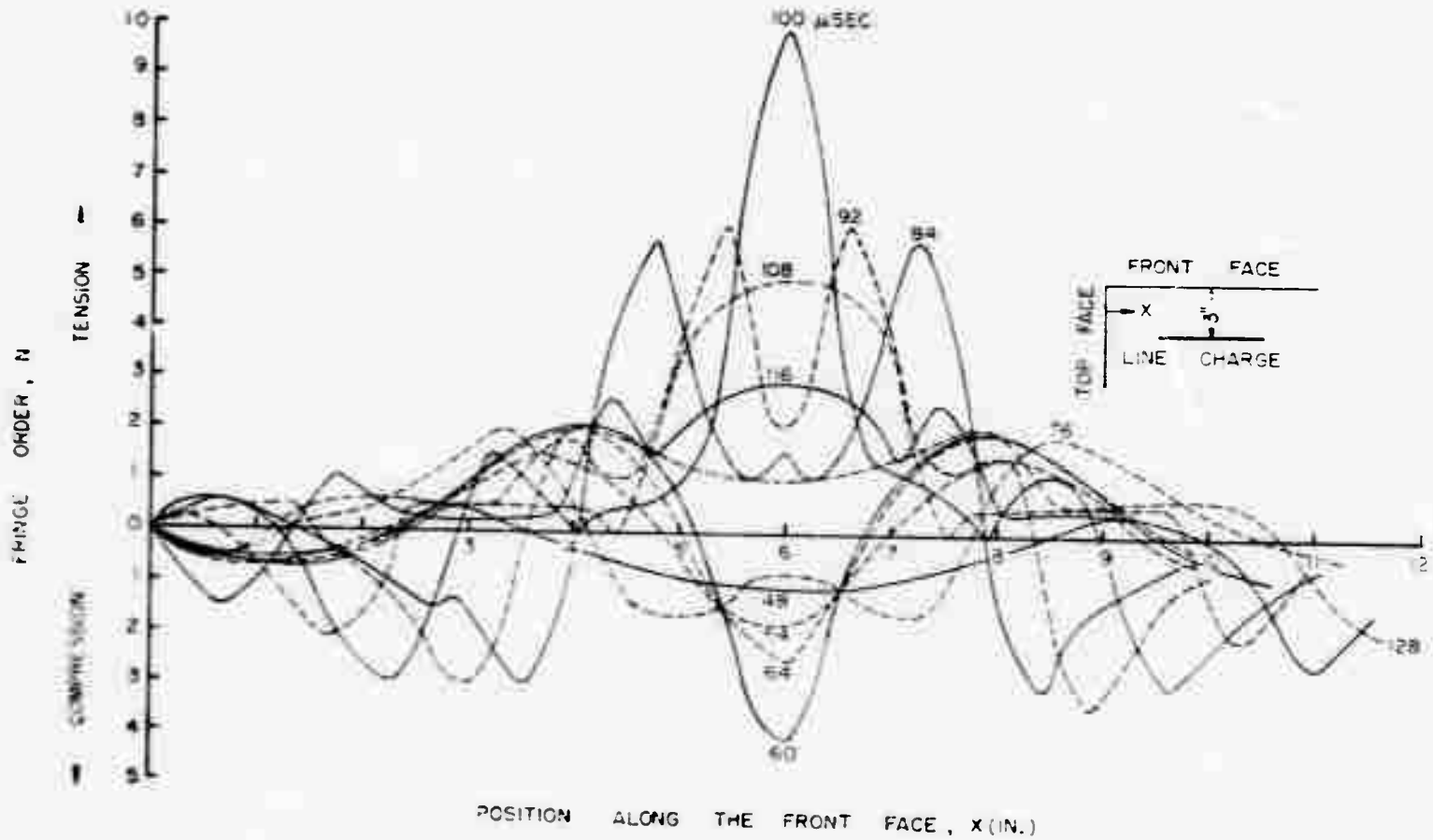


FIG. 20. FRINGE ORDER ALONG THE FRONT FACE AS A FUNCTION OF POSITION AND TIME ( s = 3 IN )

incident shear wave, S, by the reflected shear wave, SS, has now produced a maximum fringe order of 10 on the front face.

An examination of the changes in the fringe order along the normal to the front face makes it possible to identify the individual reflected stress waves which reinforce the incident shear wave. In Fig. 21, the variation of the fringe order, along the line normal to the front face and passing through the center of the line charge, is shown for selected times. The isochromatic fringe patterns illustrating the important features of stress wave interaction are presented in Fig. 22. For clarity, the following discussion is divided into four parts.

(i) Incident S wave uninfluenced by the reflected stress waves:

As shown in Fig. 21, at 86 μsec. the incident shear wave, S, shows a peak of 8.5 fringes at 2 in. from the free boundary. The incident dilatational wave, P, has produced a shear wave, PS, which shows a maximum fringe order of 4 at 3/8 in. from the front face. Both the S and the PS waves are moving towards each other, as shown by the curve for 92 μsec. At this time the PS wave has increased in amplitude to 4.5 fringes at about 5/8 in. from the front face and the peak of the S wave has shifted to 1-7/8 in. with practically no decrease in amplitude. The fringe pattern corresponding to 92 μsec. is shown in the first frame in Fig. 22.

(ii) Incident S wave reinforced by the PP wave: The curve, in Fig. 21, corresponding to 98 sec. shows that the S wave has a maximum of only 6.5 fringes, compared to 8.5 at 92 μsec.

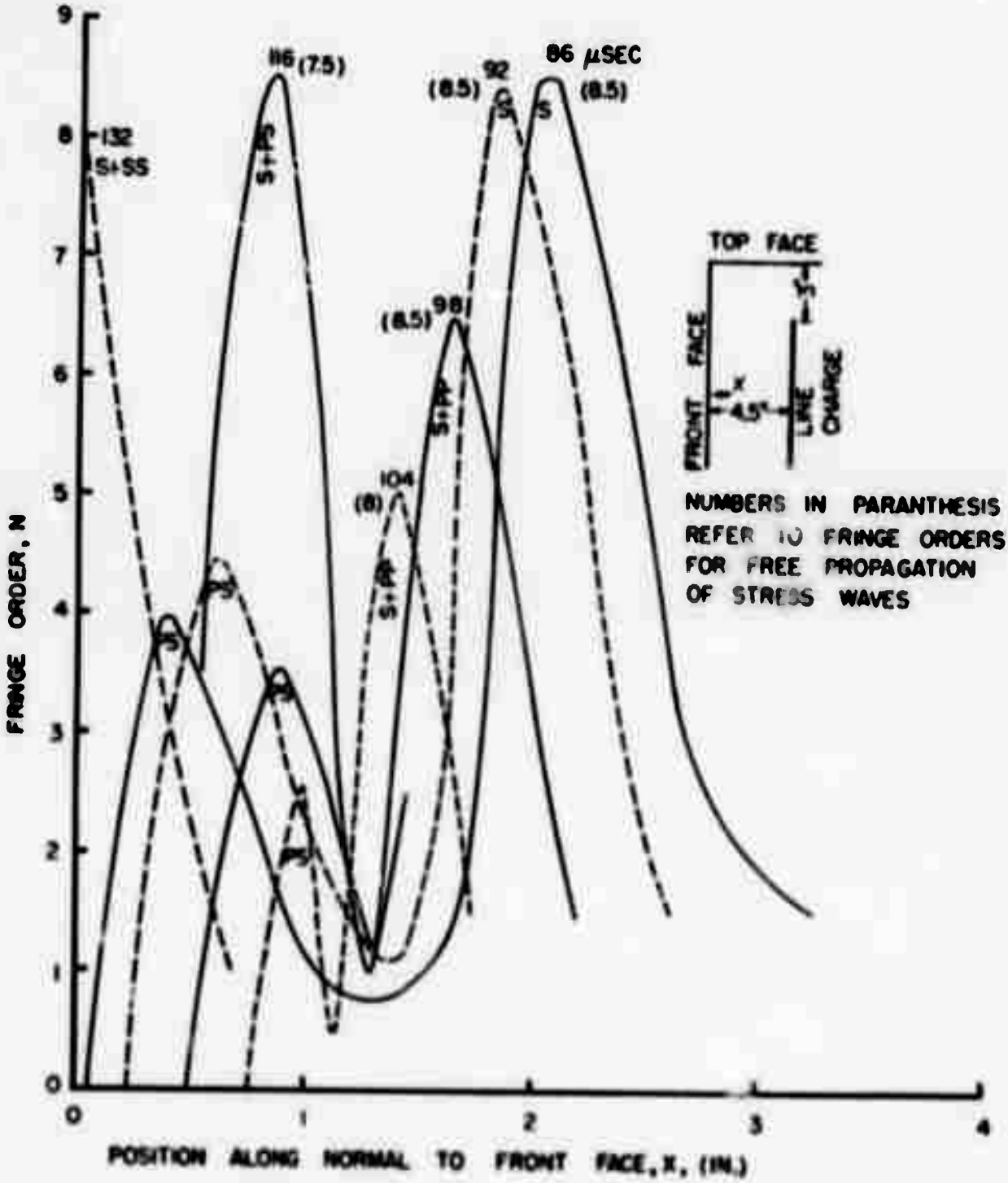


FIG.21. FRINGE ORDER ALONG THE NORMAL TO THE FRONT FACE FOR SELECTED TIMES ( S = 4.5° )

FIG.22 SELECTED FRINGE PATTERNS SHOWING THE REFLECTION PROCESSES(s=4.5 in.)

The fringe pattern corresponding to 98 μsec. is shown in the second frame in Fig. 22. From this frame, the S wave has a maximum fringe order of 8.5 on the right side of the line charge where there is no interaction. Thus the drop in the intensity of the S wave from 92 μsec. to 98 μsec. is too sudden to be due to natural attenuation. The cause of this decrease in the S wave fringe order is the reinforcement by the PP wave. The effect is similar to that described in connection with the full-plane experiments where the interaction between two P waves resulted in an increase in individual stress magnitudes but also in a decrease in the principal stress difference.

The stress state due to the shear wave, as shown in Fig. 23 (a), is composed of equal tension and compression in two perpendicular directions. While the P wave is associated with a state of biaxial compression, the PP wave produces a state of biaxial tension. Thus, when the PP wave interacts with the S wave, the individual stress magnitudes in Fig. 23(b) are algebraically increased but the resulting principal stress difference is less than that due to the S wave alone. The isochromatic fringe order, N, being directly proportional to the principal stress difference, also drops. The decrease in the fringe orders associated with the S and the PS waves continues up to 104 μsec.

(iii) <u>Incident S wave reinforced by the PS wave</u>: At a time corresponding to 116 sec., as shown in Fig. 21, the incident

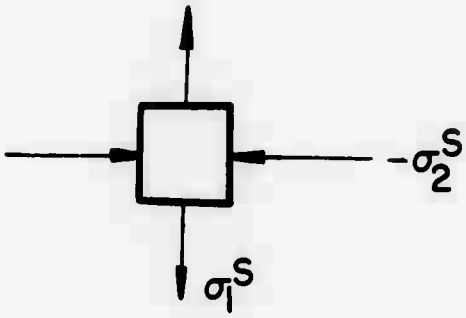


$$\sigma_1 - \sigma_2 = \sigma_1^S + \sigma_2^S$$

(A) STRESS STATE DUE TO S WAVE

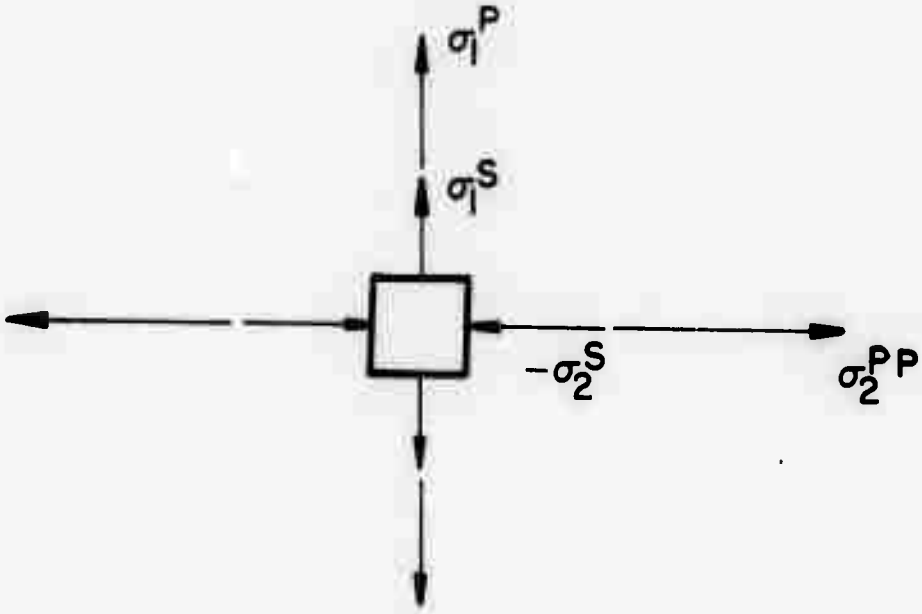


$$\sigma_1 - \sigma_2 = (\sigma_1^S + \sigma_1^{PP}) - (\sigma_2^{PP} - \sigma_2^S) = \sigma_1^S + \sigma_2^S - (\sigma_2^{PP} - \sigma_1^{PP}) < (\sigma_1^S + \sigma_2^S)$$

(B) STRESS STATE DUE TO REINFORCEMENT OF S WAVE BY THE PP WAVE

FIG. 23. REINFORCEMENT OF INCIDENT SHEAR(S) WAVE BY THE REFLECTED DILATATIONAL (PP) WAVE

S wave and the reflected shear wave due to incident P wave, the PS wave, reinforce each other. The resulting fringe pattern, shown in the third frame of Fig. 22, exhibits a maximum fringe order of 8.5. In the absence of the front face, as shown in the right half of the frame for 116 μ sec. in Fig. 22, the peak fringe order due to the S wave alone is 7.5.

(iv) Incident S wave reinforced by the SS wave: The fringe order at the front face at 132 μ sec., as shown in Figs. 21 and 22, is 8 and is due to the reinforcement of the S wave by the SS wave. In the frame corresponding to 132 μ sec., for s = 4.5 in., the stress waves have propagated out of the field on the side of the line charge opposite to the front face. Therefore, the reinforcement of the S wave by its own reflected shear wave or SS wave, is illustrated in the case of $s$ = 3 in.

The first frame in Fig. 24, corresponding to 92 μ sec. shows a maximum fringe order of 10 for the reinforced S wave near the front face and 9 for the undisturbed S wave on the opposite side of the line charge. This increase in the stress wave intensity is due to the reinforcement of the incident shear wave by the PS wave. The next frame at 100 μ sec. shows that the crests of the S waves, on either side of the line charge, have moved 0.3 in. compared to the previous frame. While the S wave on the right side of the line charge has attenuated to 8 fringes, the S wave

Reproduced from best available copy.

FIG.24 REINFORCEMENT OF THE INCIDENT SHEAR (S)WAVE BY THE REFLECTED SHEAR WAVES(PS AND SS),s=3 in.

at the front face still shows a peak of 10 fringes. The reason is that while the S wave (already reinforced by the PS wave) did attenuate in travelling the 0.3 in. distance to the front face, it has been reinforced by its own reflected shear wave.

The tensile component of the S + PS combination, corresponding to a time of 116 μ sec. in Fig. 21, produces sub-surface tension in the material and results in the phenomenon known as "scabbing" in materials which have a low tensile strength. Because of the importance of this sub-surface phenomenon, the variation of fringe order along a line 0.3 in. below the front face, for the case of s = 3 in. is shown in Fig. 25. A fringe order maximum of 10 is attained at a point directly in line with the center of the line charge and is due to the reinforcement of the S wave by the PS wave. If the tensile stress associated with the state of pure shear exceeds the tensile strength of the material, then scabbing occurs.

Comparison of the three quarter plane experiments:

As mentioned in the comparison of the different ignition procedures in the full plane experiments, not only the stress magnitudes but also the extensiveness of the highly stressed regions must be considered for applications involving material breakage, such as rock blasting. In this section a brief comparison of the three quarter plane experiments, based on these factors, is given.

The maximum isochromatic fringe order at the front

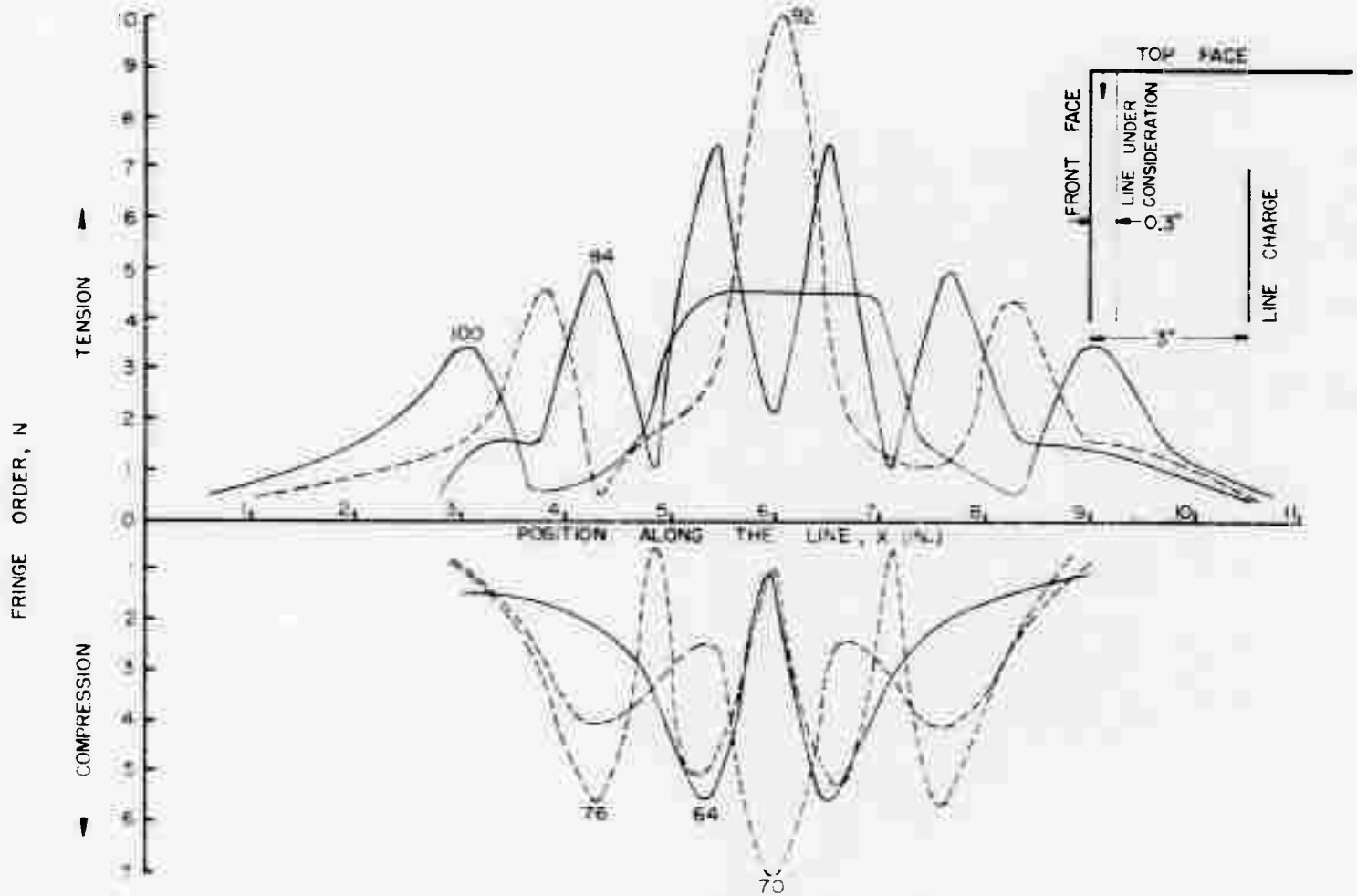


FIG. 25. FRINGE ORDER ALONG A LINE 0.3 IN. BELOW THE FRONT FACE AS A FUNCTION OF POSITION AND TIME (s= 3 IN.)

face is shown in Fig. 26 as a function of the spacing between the line charge and the front face. As explained before, this maximum fringe order is due to the reinforcement of the incident shear wave, S , by the reflected shear wave, SS. When the spacing, s, is reduced from 6 in. to 4.5 in., the maximum fringe order is doubled from 4 to 8. But a further reduction in s from 4.5 in. to 3 in. results only in an increase from 8 to 10 fringes. The reason for the diminishing slope of the curve for decreasing values of s, in Fig. 26, is illustrated in Fig. 27, where selected fringe patterns for the double end ignition in a full plane are presented. In the first frame the two shear waves due to the two halves of the line charge have reinforced each other and the resulting maximum fringe order of about 7 occurs at 2 in. from the line charge. In the second and third frames the crest of the shear wave has moved to 2.5 in. and 2.7 in. respectively, without a decrease in intensity. In the last frame, the maximum fringe order is still 6.5 although now occurring at 3.7 in. from the line charge. Thus, between the first and the last frames, although the shear wave has travelled almost 2 in., the maximum fringe order associated with the wave has dropped by only 0.5. The slow attenuation of the shear wave between 2 and 5 in. from the line charge is responsible for the flattening of the curve in Fig. 26 between 3 and 4.5 in.

The spatial disposition of the stress wave peaks due to the PS and the S waves for the three values of s is

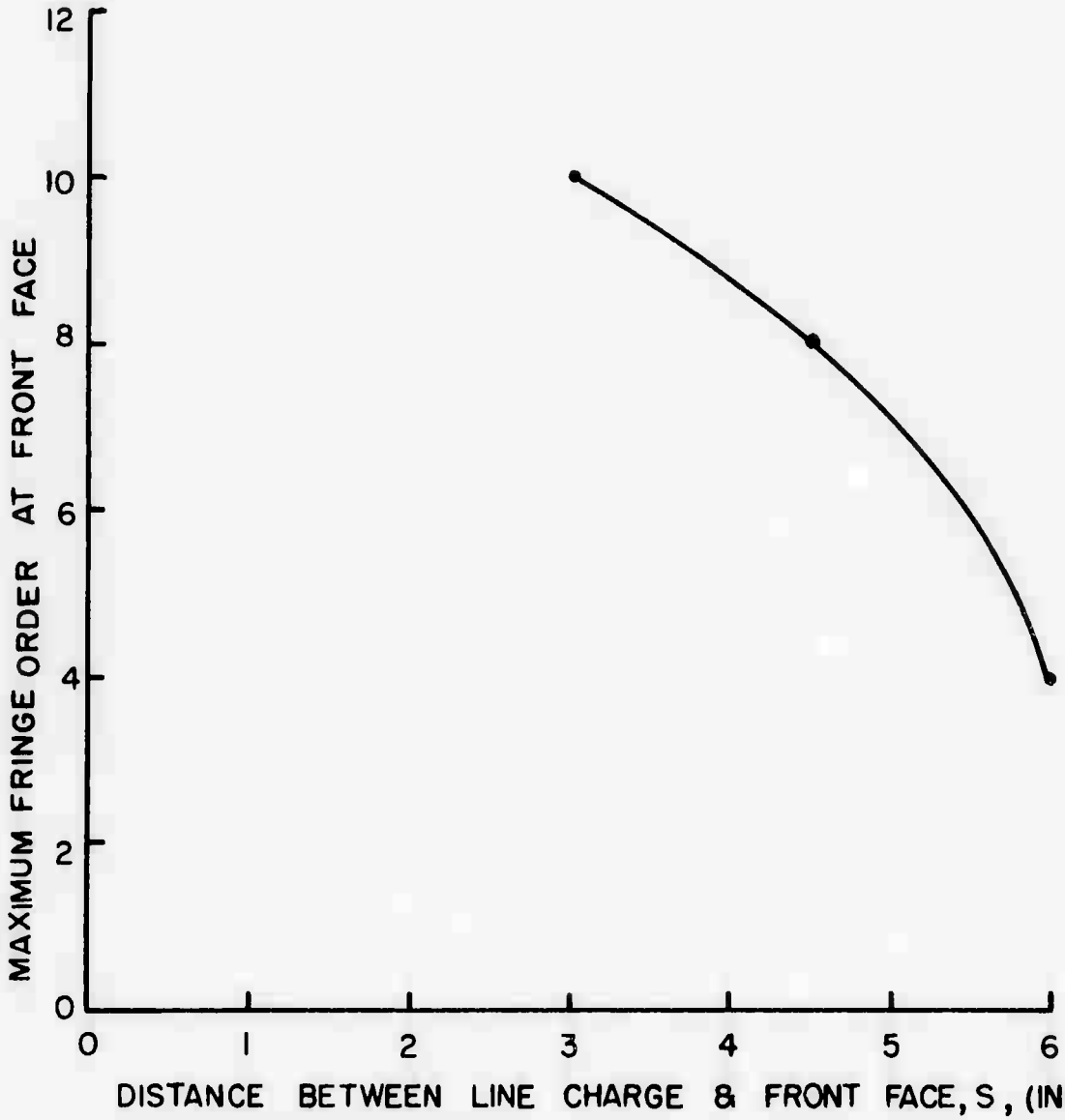


FIG. 26. MAXIMUM FRINGE ORDER AT THE FRONT FACE AS A FUNCTION OF THE DISTANCE BETWEEN THE FRONT FACE AND THE LINE CHARGE (S)

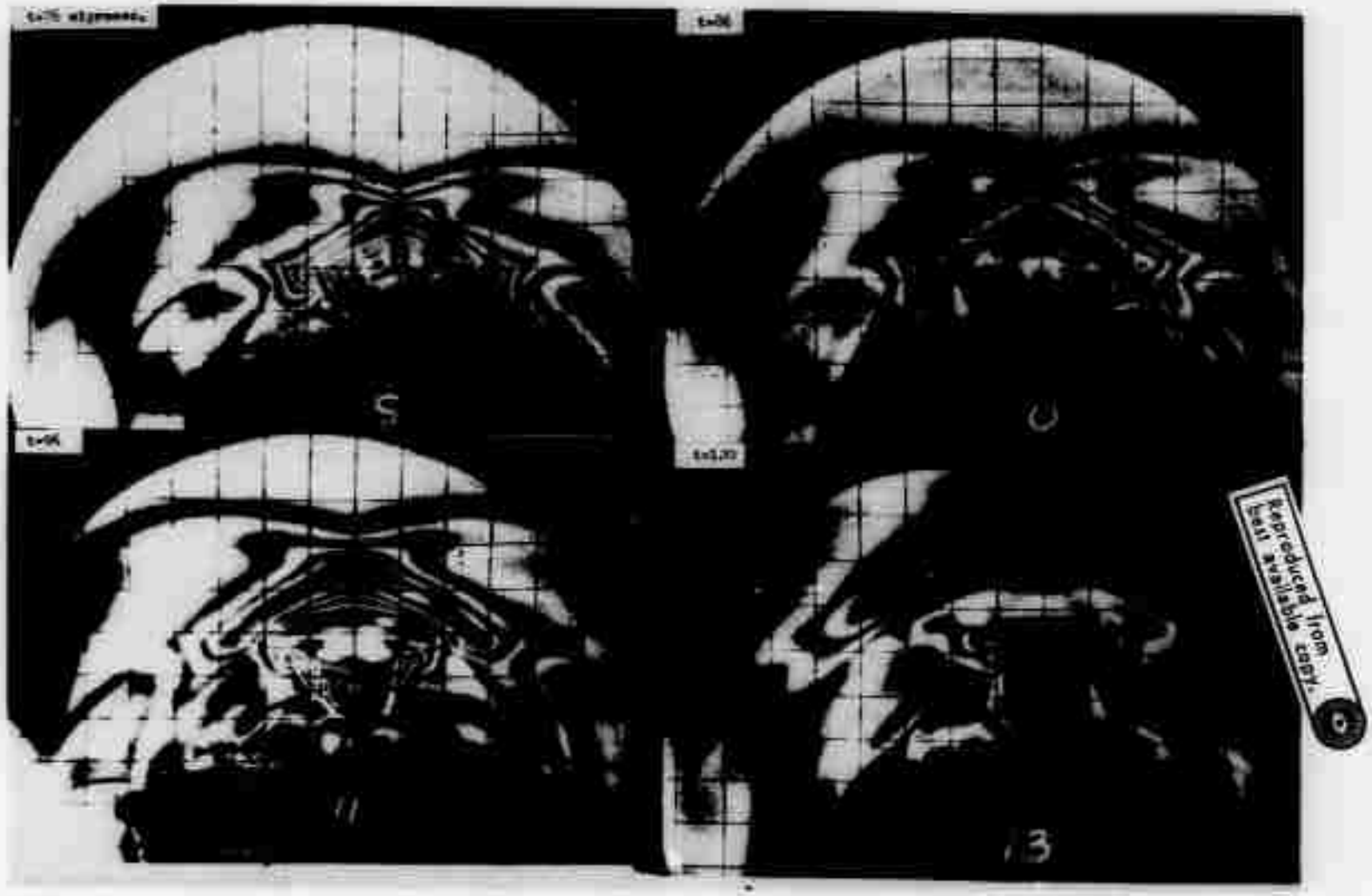


FIG.27 FRINGE PATTERNS ILLUSTRATING THE GRADUAL ATTENUATION OF SHEAR WAVE FOR DOUBLE END IGNITION

illustrated in Fig. 28. In the first frame, corresponding to s = 6 in., the crest of the S wave (already reinforced by the PS wave) exhibits a maximum fringe order of 4.5 and the PS wave shows a maximum of 3, the two crests separated by a distance of 3 in. along a line 1 in. away from the front face. In the second frame, corresponding to s = 4.5 in., the S wave shows a maximum fringe order of 9, the PS wave has a maximum of 3.5 and the two maxima are separated by a distance of 2 in. along a line parallel to the front face. When s = 3 in., as shown in the third frame, the maximum fringe orders for the S and the PS wave are 10.5 and 4.5 respectively and the distance separating them is 1 in. only, parallel to the boundary.

Thus, changing the spacing between the line charge and the front face results not only in different amplitudes of the stress waves but also in different spatial distributions of the crests of the stress waves. In evaluating the distribution of the stress wave peaks, it is necessary to consider the requirements of a line charge and the properties of the material used. It is obvious that if the peaks of the stress waves are too far apart, cracks will be induced in the material but these cracks will not always join to fragment the material. On the other hand, if the stress wave peaks occur too close to each other, the material will be damaged over a small region. An optimum spacing between the maxima due to the stress waves depends on the properties of the material dealt with.

FIG.28 FRINGE PATTERNS ILLUSTRATING THE SPATIAL DISTRIBUTION OF SHEAR STRESS MAXIMA FOR DIFFERENT VALUES OF t

# V. CONCLUSIONS

Summary of Results:

Three different ignition methods for a line charge of explosive - ignition at the center, ignition at one end and simultaneous ignition at both ends - were investigated. These ignition procedures were compared on the basis of the stress waves produced when the line charge was ignited in a full plane model of a photoelastic material. The line charge produced, for all three methods of ignition, two types of stress waves, the dilatational (P) wave and the shear (S) wave. The dilatational wave was not considered as a factor of comparison between the ignition procedures because the stress state associated with the P wave is biaxial compression which is not significant in producing fracture in brittle materials. The magnitude of the shear stress associated with the shear wave and the extensiveness of the high shear stress regions were considered in comparing the ignition methods. Based on these criteria, igniting the line charge at its center was found to be the least effective ignition procedure. Single end ignition and double end ignition were comparable in their effectiveness, both in terms of the magnitude of the shear stresses and in terms of the areas of high shear stress.

In the second series of experiments, the mechanism of reflection and reinforcement of stress waves from a free boundary, when this boundary was parallel to the line charge, was investigated. The ignition procedure employed

in these tests was that of double end ignition. Results from three dynamic photoelastic tests were presented, with the spacing between the line charge and the free boundary equal to 3, 4.5 and 6 inches. The two incident stress waves, P and S, produced four reflected stress waves, PP, PS, SP and SS. For reasons explained in the case of the full plane experiments, only the incident shear wave was studied in the quarter plane experiments. The reinforcement of the S wave by the PP, PS and SS waves was considered. While the interaction of the S wave with the PP wave resulted in a decrease in the isochromatic fringe order, reinforcement by the PS and SS waves produced significant increases in the fringe order. Interaction of S and PS waves was responsible for subsurface stress peaks which could cause scabbing. Reinforcement of S wave by the SS wave produced high shear stresses at the free boundary itself. As the spacing between the line charge and the free boundary was reduced, the intensities of the S and the PS waves increased and the peaks of these stress waves were brought closer. An optimum spacing depends upon the requirements of extensiveness of fracture and the degree of fragmentation.

Future Work:

Dynamic photoelastic experiments, of the type described in this study, can generate very useful information. The conclusions from the full plane experiments, that center ignition of the line charge is the least effective and that single and double end ignition methods

are comparable in their effectiveness, belong to this class of information. However, if the ultimate objective is to cause fracture and fragmentation in brittle materials, it is necessary to conduct tests with brittle models. In the following discussion three classes of experiments are suggested to generate information in the laboratory before the results are applied in the field.

(i) Photoelastic study of stress waves:

This series of experiments is an extension of the tests conducted in this study. In the case of the full-plane, the line charge can be ignited at more than two points simultaneously (for instance at the two ends and at the center). In the case of the quarter plane, the line charge can be oriented at different angles to the free boundary and an optimum orientation can be found for single end ignition. These results may necessitate a fresh comparison of the single and double end ignition procedures.

(ii) Photoelastic study of stress waves and fracture:

In the case of brittle materials, stress waves induce fracture which in turn influences the stress waves. This interaction between stress waves and fracture can be studied if glass is used as the photoelastic material.

(iii) Laboratory study of fracture:

Verification of the conclusions from the two series of experiments listed above can be conveniently accomplished in the laboratory by testing slabs of material which are encountered in the field.

# APPENDIX A

## FRINGE PATTERNS

Reproduced from best available copy.

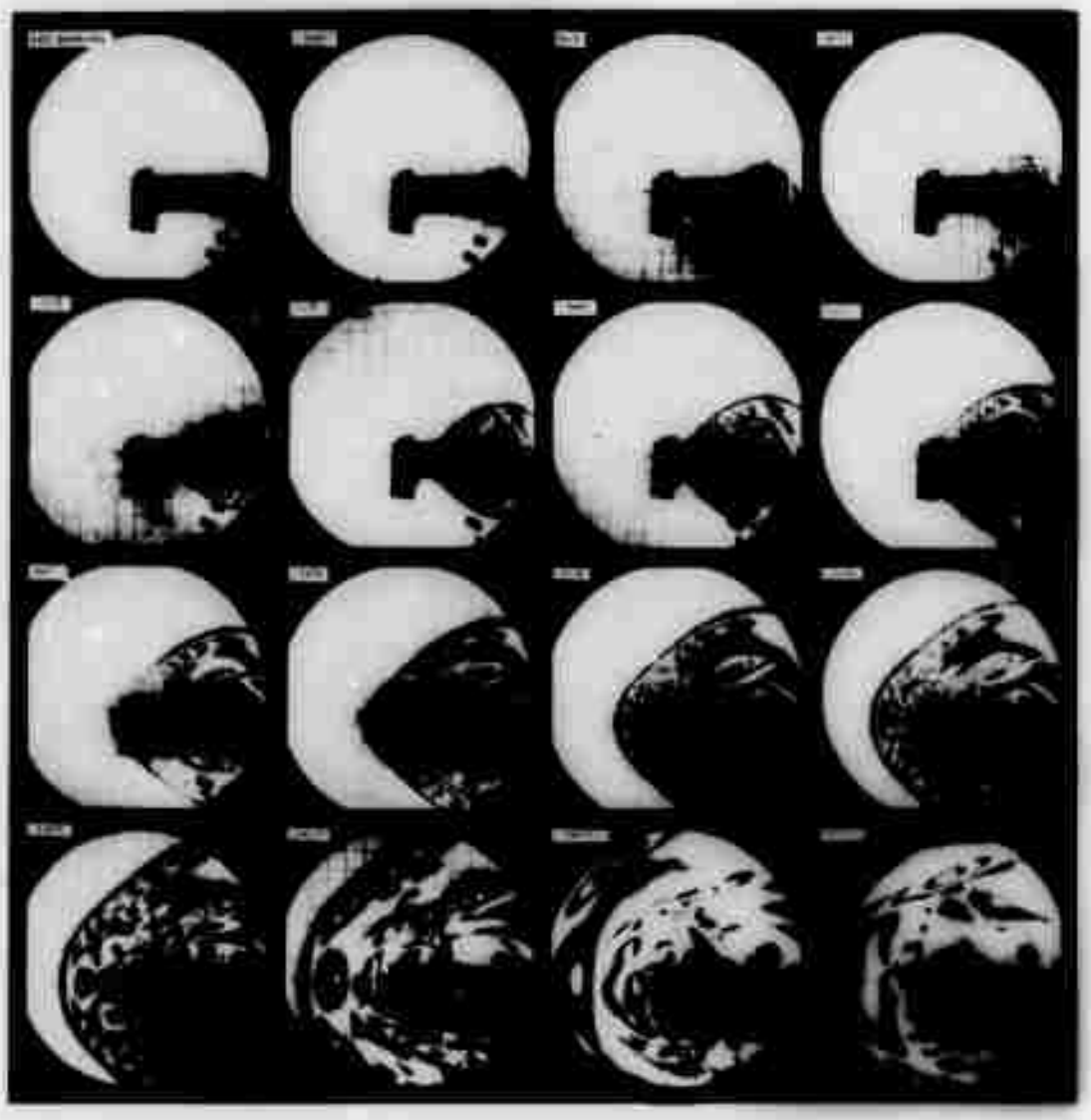

FIG.A-1 ISOCHROMATIC FRINGE PATTERNS FOR SINGLE END IGNITION OF A LINE CHARGE IN A FULL PLANE

Reproduced from best available copy.

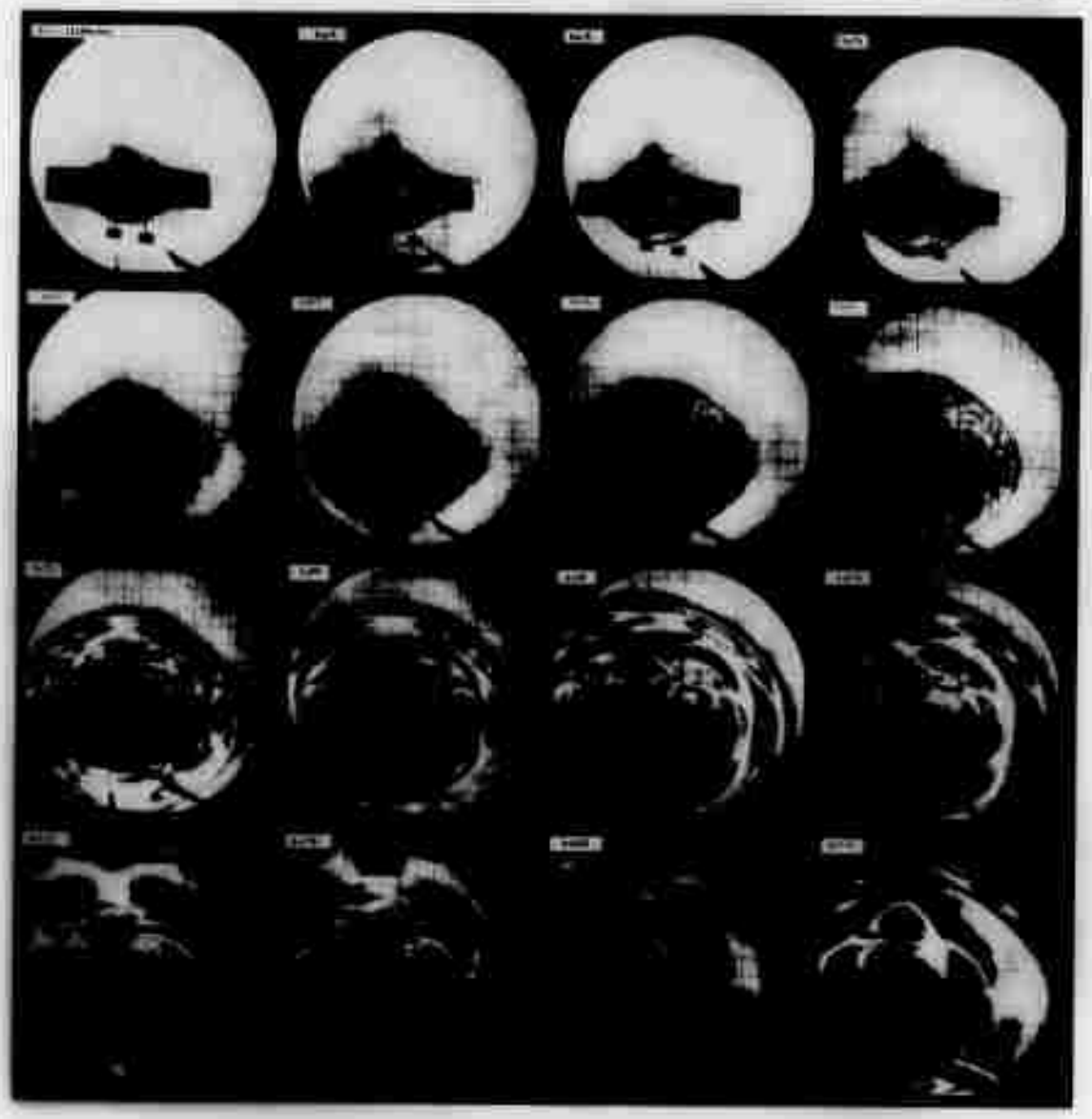

FIG.A-2 ISOCHROMATIC FRINGE PATTERNS FOR CENTER IGNITION OF A LINE CHARGE IN A FULL PLANE

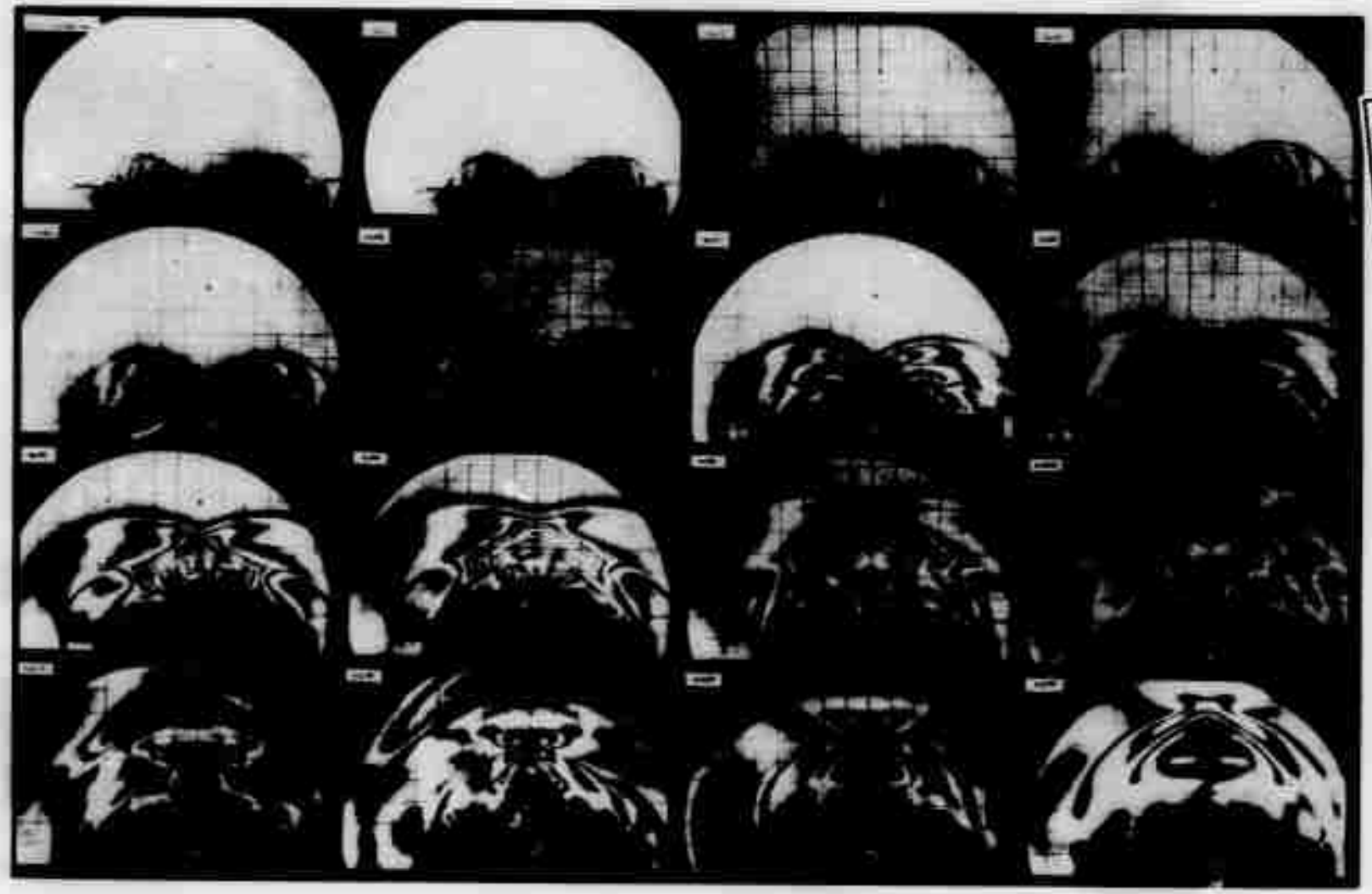

Reproduced from best available copy.

FIG.A-3 ISOCHROMATIC FRINGE PATTERNS FOR DOUBLE END IGNITION OF A LINE CHARGE IN A FULL PLANE

Reproduced from best available copy.

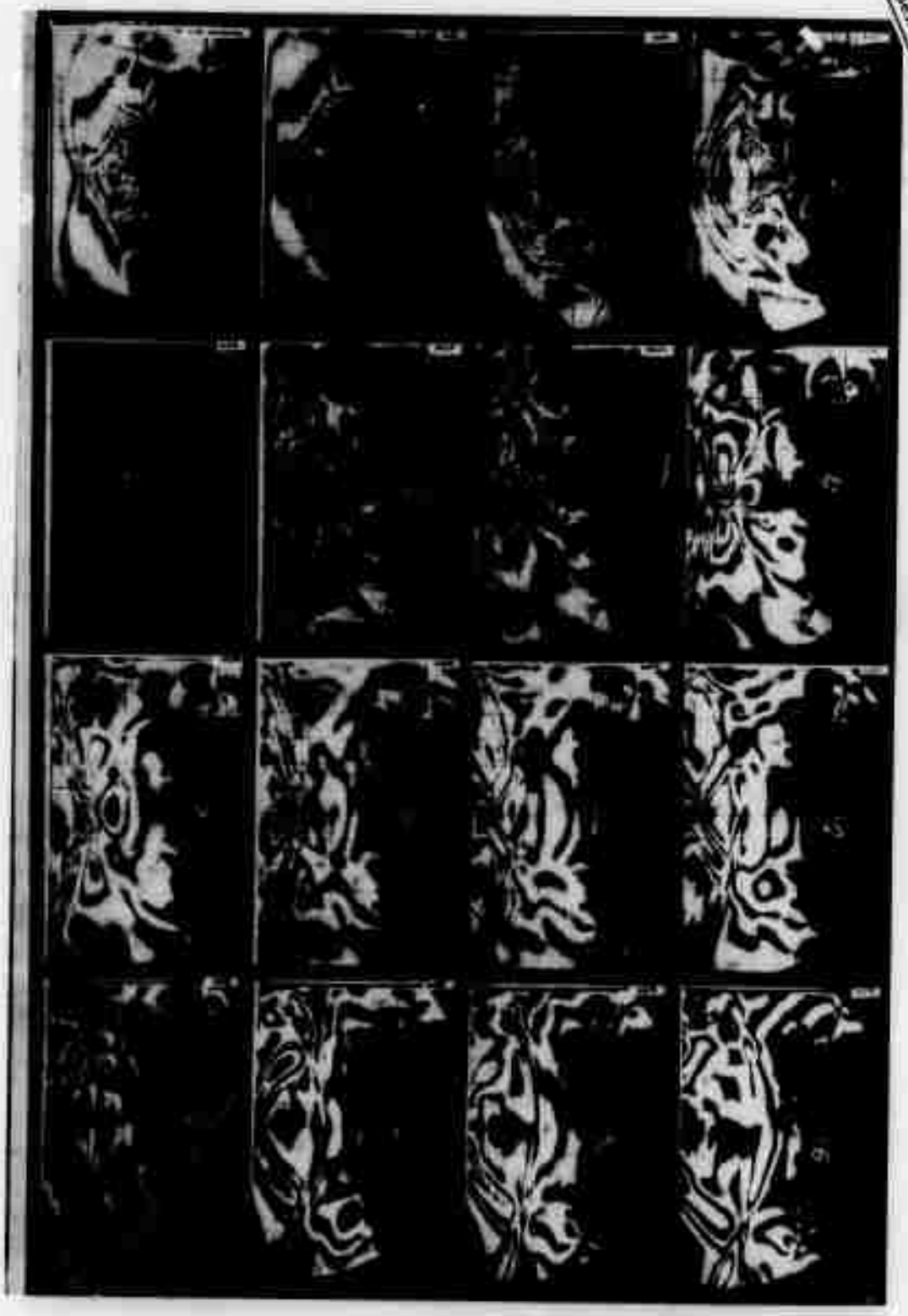

FIG.A-4 ISOCHROMATIC FRINGE PATTERNS FOR THE QUARTER PLANE EXPERIMENT WITH s=6 in.

Reproduced from best available copy.

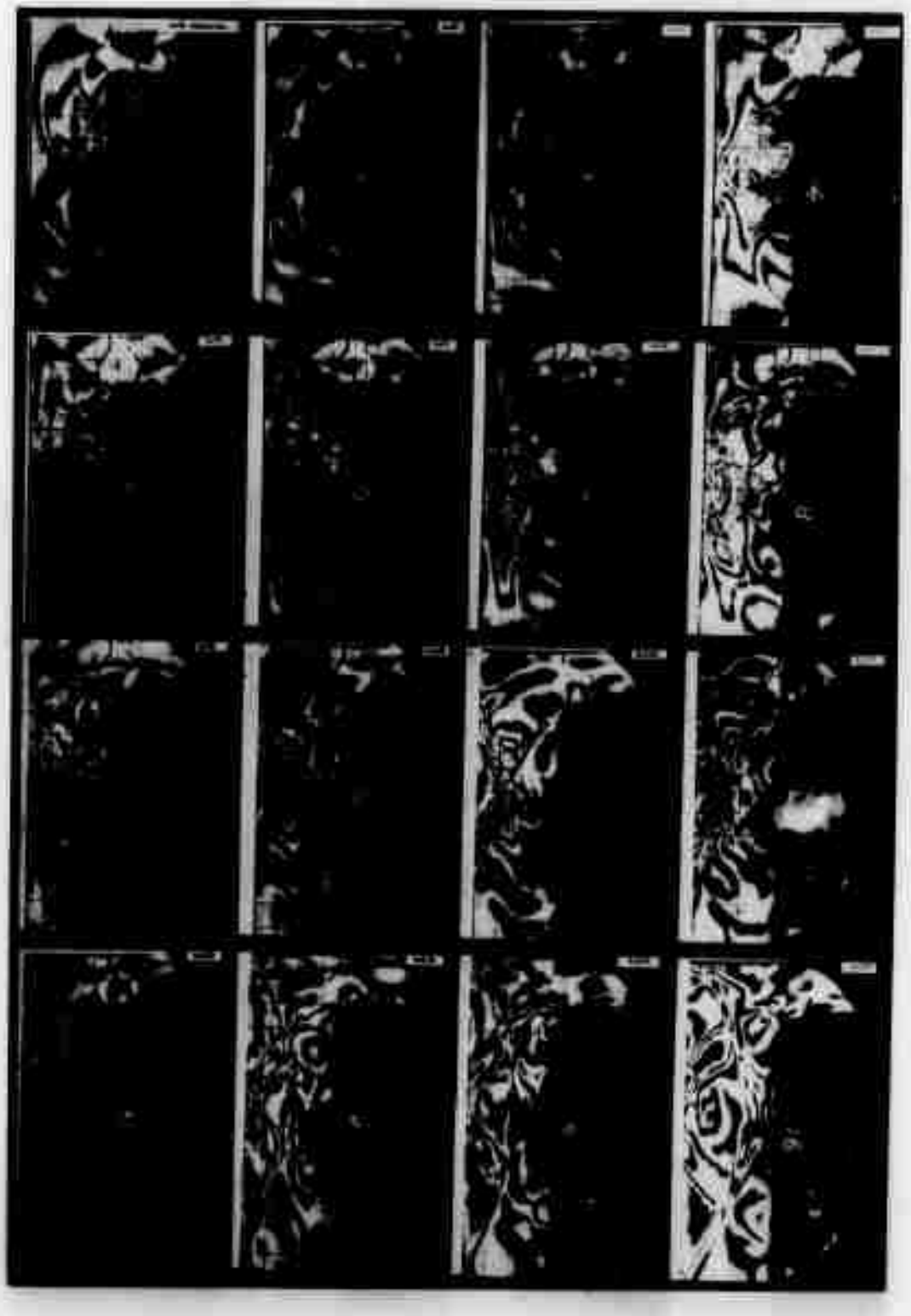

FIG.A-5 ISOCHROMATIC FRINGE PATTERNS FOR THE QUARTER PLANE EXPERIMENT WITH s=4.5 in.

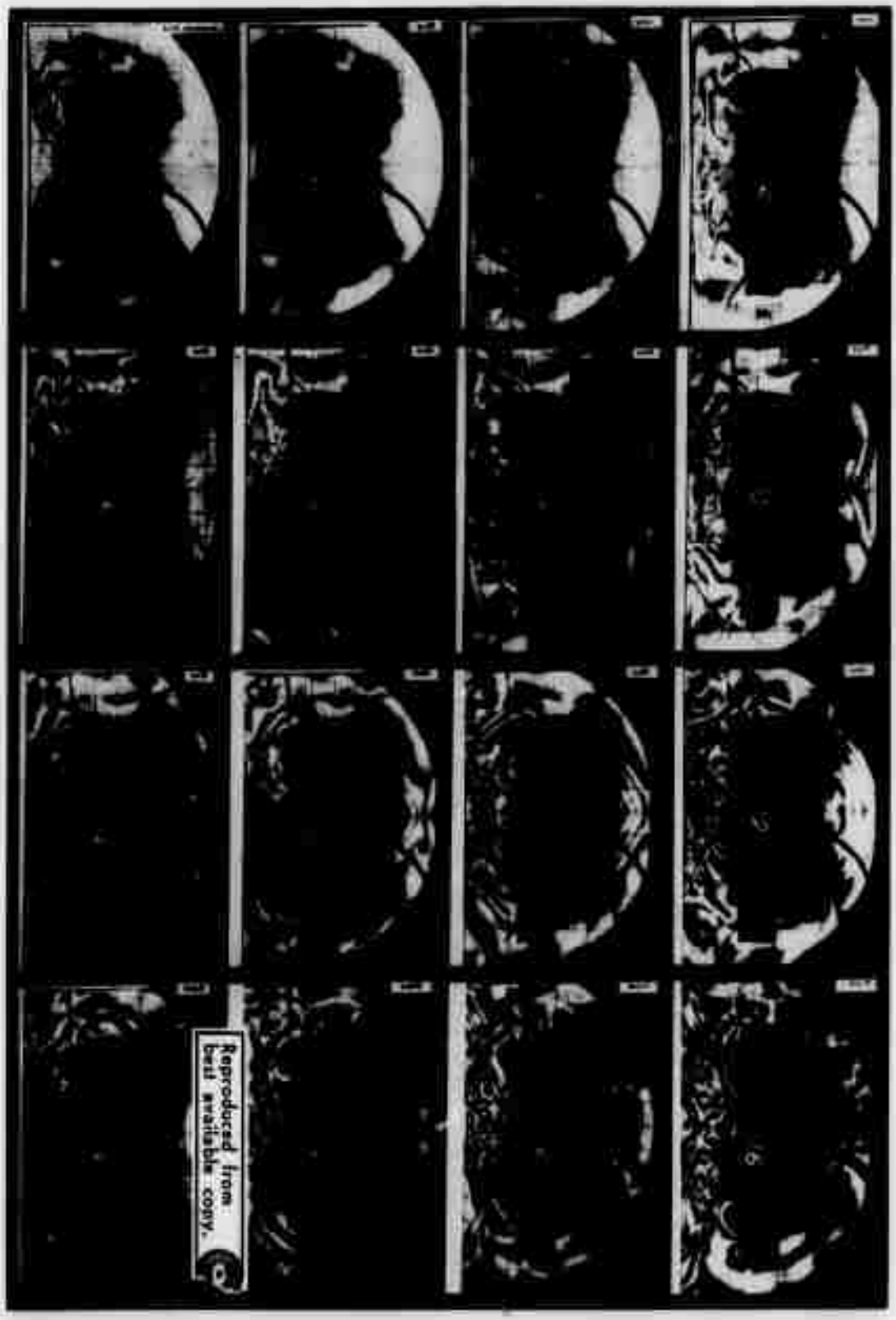


FIG.A-6 ISOCHROMATIC FRINGE PATTERNS FOR THE QUARTER PLANE EXPERIMENT WITH s=3 in.

## BIBLIOGRAPHY


1. Tandanand, S., and Hartman, H. L., "Investigation of Dynamic Failure by High-Speed Photography," Proceedings of the Fifth Rock Mechanics Symposium, Pergamon Press, New York, 1963.

2. Dally, J. W., and Khorana, S. S., "A Dynamic Photoelastic Investigation of Stress Wave Propagation in a Half-Plane with Multiple Dilatational Sources," Semi-Annual Technical Report, Illinois Institute of Technology, August, 1971.

3. Reinhardt, H. W., and Dally, J. W., "Dynamic Photoelastic Investigation of Stress Wave Interaction with a Bench Face," Trans. Soc. of Mining Engineers, AIME, Vol. 250, March, 1971, pp. 35-42.

4. Dally, J. W., and Riley, W. F., Experimental Stress Analysis, McGraw Hill, New York, 1965, pp. 165-183.